Space-time-resolved Breit-Wheeler process for a model system

Y. Lu, N. Christensen, Q. Su, and R. Grobe

Phys. Rev. A **101**, 022503 — Published 12 February 2020

DOI: 10.1103/PhysRevA.101.022503

Space-time resolved Breit-Wheeler process for a model system

Y. Lu(1,2), N. Christensen(2), Q. Su(2) and R. Grobe(2)

(1) College of Physical Sciences, University of Chinese Academy of Sciences, Beijing 100190, China

(2) Intense Laser Physics Theory Unit and Department of Physics Illinois State University, Normal, IL 61790-4560 USA

We study the creation process of an electron-positron pair as a result of the collision between two incoming photons with full spatial and temporal resolution. The dynamics of the four involved particles is described by a simplified model based on a Yukawa Hamiltonian in one spatial dimension. This quantum field theoretical approach permits us to go beyond the usual external field approximation and to study the depletion of the two colliding photon wave packets due to the back-reaction of the created electron-positron pair. If the spatial extension of the incoming photons is sufficiently narrow, we predict an interesting blue shift with regard to the optimum incoming photon momentum that can maximize the pair creation yield close to the threshold momentum.

1. Introduction

In 1934 a pioneering work by G. Breit and J.A. Wheeler [1] proposed for the first time that the collision of two highly energetic photons could lead to the creation of an electron-positron pair. This process is from a fundamental point of view very interesting, as it provides the simplest mechanism under which pure light quanta can be converted into matter therefore providing a direct manifestation of the equivalency between energy and mass. Starting in the 1960s, further studies of the pair creation process via the multiphoton absorption in strong electromagnetic fields were reported [2-5].

Due to the technical difficulty to generate gamma rays with sufficiently high intensity, this phenomenon has not been confirmed directly by experiments up to this point. However, a more complicated version of this process was realized in the famous SLAC experiment in 1997 [6], where a highly accelerated electron beam was first used to create high-energy photons via the nonlinear inverse Compton scattering mechanism [7-8]. Subsequently, these photons interacted with the same laser to generate multi-photon electron-positron pairs. As the power of the experimentally available laser fields has steadily increased over the last years, there are also plans to revisit the multi-photon Breit-Wheeler process within an all-optical environment.

Due to its fundamental significance, the process has also been studied widely from a theoretical point of view [9-14]. There are numerous interesting calculations that aim to determine the transition rates for realistic laboratory conditions, where the two counter propagating laser fields have complicated space-time profiles. Here it was proposed to generalize the usual laser-dressed final states by modified Volkov states [15] that can incorporate perturbatively spatial and temporal inhomogeneities [16-18].

In this work, the emphasis is more on the fundamental quantum field theoretical features of this basic process. We note that similar to the original Breit-Wheeler work, most theoretical treatments consider the interaction under the external field approximation, where the photons are described by a classical electromagnetic field with a predetermined spatial and periodic temporal dependence. This restriction to classical external fields prohibits the theoretical access to truly dynamical features of the photons, such as their role in particle dressing [19-21], energy shifts and other intrinsically quantum field theoretical characteristics.

The present work is different from prior studies in two respects. First, it does not approximate the two colliding photons by two time-dependent force fields with a prescribed temporal dependence, but as two fully coupled quantum field theoretical variables that are being treated on the same dynamical level as the electron and positron. Second, by superimposing states with different total momentum, we can examine the collision within the quantum field theoretical framework with space-time resolution.

This manuscript is structured as follows. In Section 2, we introduce the model system, its notation and the underlying fundamental Hamiltonian that becomes accessible to numerical simulations. In Section 3, we

reduce the dynamics to an essential state system. In Section 4, we adiabatically eliminate the intermediate three-particle states, which reduces the dynamics to an effective two-level system. We also test the range of validity of this approximation. In Section 5, we analyze the time evolution of the pair production for an infinitely extended initial two-photon state into a continuum of final electron-positron states. We also derive a Breit-Wheeler rate and compare it with the one obtained from the perturbative Fermi's Golden rule. In Section 6, we examine how the Breit-Wheeler decay rate obtained from two monochromatic photons can guide the study of the space-time resolved photon-photon scattering, where the initial state is a superposition of photons with various momenta. We examine the time-dependence of the spatial densities for the photons and the created electron-positron pairs during and after the collision. In Section 7, we summarize the work and discuss open questions. For better readability and a better focus on the physical predictions, we have shifted major mathematical derivations to three appendices.

2. The model system

In this section we briefly introduce our toy model and its notation. In order to be able to examine the photon-photon interaction from a quantum field theoretical perspective, numerous theoretical restrictions have to be made up front to make the system computationally feasible. We denote the momenta of the electrons, positrons and photons by p, q and k, respectively. The two fermions have a bare mass M and the photon is assumed to have a small mass m, whose numerical value could be chosen zero, but in order to avoid possible infra-red singularities in our computer simulations, we choose a small but finite value, $m < M$. Furthermore, we assume that the model photon has a zero spin component along the propagation direction and that the spatial dimension is restricted to only one, represented by the x-axis. We choose this simple model as it permits us to examine numerically the validity of several approximations that accompany this theoretical framework. In atomic units, where $m=\hbar=e=1$, the bare energies are given by $E_p \equiv [M^2c^4+c^2p^2]^{1/2}$ for the electrons, $E_q \equiv [M^2c^4+c^2q^2]^{1/2}$ for the positrons and by $\omega_k \equiv [m^2c^4+c^2k^2]^{1/2}$ for the photons. The fermionic momentum creation and annihilation operators fulfill the usual anti-commutator relationships, $[b(p),b(p')\dagger]_+ = \delta(p-p')$, $[d(q),d(q')\dagger]_+ = \delta(q-q')$, $[b(p),b(p')]_+ = 0$, $[d(p),d(p')]_+ = 0$, $[b(p)\dagger,b(p')\dagger]_+ = 0$, $[d(p)\dagger,d(p')\dagger]_+ = 0$, $[d(q)\dagger,b(p')]_+ = 0$, $[b(q)\dagger,d(p')]_+ = 0$, while the corresponding bosonic operators fulfill the usual commutator relationships $[a(k),a(k')]_- = 0$, $[a(k)\dagger,a(k')\dagger]_- = 0$ and $[a(k),a(k')\dagger]_- = \delta(k-k')$. The interaction energy coupling the fermionic and bosonic field operators is chosen in this model study as $V= \lambda\, c^{3/2} \int dx\, \Psi\dagger\, \sigma_3\, A\, \Psi$, with the 2×2 Pauli matrix σ_3. In Appendix A, we derive the form for the Hamiltonian H. For our numerical purposes

it is represented on the discretized numerical grid as

$$H = \Sigma_p E_p\, b(p)^\dagger\, b(p) \;+\; \Sigma_q E_q\, d(q)^\dagger\, d(q) \;+\; \Sigma_k \omega_k\, a(k)^\dagger\, a(k) \;+\; \Sigma_{n=18} V_n \qquad (2.1)$$

where the eight fundamental interactions of our model of qed are given by

$$V_1 = g\;\; \Sigma_p \Sigma_k\, \Gamma^{UU}(p,p-k,k)\;\; b_p^\dagger\, b_{p-k}\, a_k \qquad (2.2a)$$

$$V_2 = g\;\; \Sigma_p \Sigma_k\, \Gamma^{UU}(p,p+k,k)\;\; b_p^\dagger\, b_{p+k}\, a_k^\dagger \qquad (2.2b)$$

$$V_3 = g\;\; \Sigma_p \Sigma_k\, \Gamma^{UD}(p,p-k,k)\;\; b_p^\dagger\, d_{-p+k}^\dagger\, a_k \qquad (2.2c)$$

$$V_4 = g\;\; \Sigma_p \Sigma_k\, \Gamma^{UD}(p,p+k,k)\;\; b_p^\dagger\, d_{-p-k}^\dagger\, a_k^\dagger \qquad (2.2d)$$

$$V_5 = g\;\; \Sigma_p \Sigma_k\, \Gamma^{DU}(p+k,p,k)\;\; d_{-p-k}\, b_p\, a_k \qquad (2.2e)$$

$$V_6 = g\;\; \Sigma_p \Sigma_k\, \Gamma^{DU}(p-k,p,k)\;\; d_{-p+k}\, b_p\, a_k^\dagger \qquad (2.2f)$$

$$V_7 = g\;\; \Sigma_p \Sigma_k\, \Gamma^{DD}(-p,-p-k,k)\;\; d_p\, d_{p+k}^\dagger\, a_k \qquad (2.2g)$$

$$V_8 = g\;\; \Sigma_p \Sigma_k\, \Gamma^{DD}(-p,-p+k,k)\;\; d_p\, d_{p-k}^\dagger\, a_k^\dagger \qquad (2.2h)$$

where for notational convenience we denote the discrete momenta from now on as subscripts. We have introduced the coupling constant $g \equiv \lambda\, \Delta p^{1/2}\, c^{5/2}$. We have absorbed the parameters Δp and $c^{5/2}$ into g only for notational simplicity. The concrete dynamical scenario of the Breit-Wheeler effect will suggest that for renormalization purposes λ (and not g) is the relevant coupling constant, which has the unit of a mass. This is also fully consistent with prior work with this Hamiltonian [22], where the bound state energy for a fixed λ became independent of (sufficiently small) Δp.

The interactions of Eq. (2.2) represent the well-known eight processes:
$e_- + \omega \to e_-$, $e_- \to e_- + \omega$, $\omega \to e_- + e_+$, $0 \to e_- + e_+ + \omega$, $e_- + e_+ + \omega \to 0$, $e_- + e_+ \to \omega$, $e_+ + \omega \to e_+$, and $e_+ \to e_+ + \omega$. We show in Appendix A, that the four different types of coupling functions Γ^{UU}, Γ^{DD}, Γ^{UD} and Γ^{DU} can be related to only the two functions

$$\Gamma^{UU}(p,p',k) \equiv [E(p)E(p') + M^2c^4 - pp'c^2]^{1/2}\, [8\pi\omega(k)\, E(p)\, E(p')]^{-1/2} \qquad (2.2i)$$

$$\Gamma^{UD}(p,q,k) \equiv \mathrm{sign}(p/q+1)\, [E(p)E(q) - M^2c^4 + pqc^2]^{1/2}\, [8\pi\omega(k)\, E(p)\, E(q)]^{-1/2} \qquad (2.2j)$$

These are the results of the scalar product among the Dirac spinors and act as natural cut-off functions as they decrease with increasing momenta p and k.

As a consequence of the translation invariance, the Hamiltonian commutes with the total momentum operator $\Sigma_p\, p\, b(p)^\dagger\, b(p) + \Sigma_q\, q\, d(q)^\dagger d(q) + \Sigma_k\, k\, a(k)^\dagger\, a(k)$. As we will see below, the resulting conservation of the total momentum simplifies our analysis significantly, even though a pair of uncorrelated spatially localized photon wave packets cannot take a sharp momentum.

We should point out that despite the approximations concerning the spatial dimensions, the fermions' spin directions, and non-vanishing mass of the model photons, due to its fundamental character this Hamiltonian (and its reduced versions) has been studied in a wide variety of contexts. For example, to name a few, this includes the examination of the origin of attractive and repulsive interfermionic forces due to the exchange of intermediating photons [23], the evolution of bare electrons into physical electrons under photon emission [24,25], a space-time resolved Compton scattering [26], the formation of fermion bound states in the perturbative and also Borel summable non-perturbative regimes [22,27,28].

The Hamiltonian has the three adjustable parameters including the two bare masses m and M and the coupling constant λ. These free parameters need to be chosen appropriately such that the eigenvalues of H associated with the physical single fermion and photon would take the correct energy. These renormalization constants depend on the largest momentum included in the calculations. In this work, we delay the mass and charge renormalization and perform it only after the reduction of the Breit-Wheeler dynamics to a Hilbert space spanned by just the dynamically relevant states.

3. Reduction to an essential state system with a continuum of final states

In this section, we assume that the initial state for our system is given by two spatially infinitely-extended bare photons of sharp momentum K_1 and K_2, i.e. $|\Psi(t=0)\rangle = |K_1K_2\rangle$. This two-particle state is normalized based on momentum, i.e. $\langle K_1K_2|K_3K_4\rangle = \delta_{K_1K_3}\, \delta_{K_2K_4}$, where our notation always assumes $K_1 \leq K_2$ and $K_3 \leq K_4$. As this state is not an energy eigenstate, its corresponding bare energy (associated with the interaction-free Hamiltonian) $\omega_1 + \omega_2$ can play a role at most in the weak-coupling limit. As the total momentum is conserved, this initial state couples only to those subsets of states, whose momentum is precisely equal to K_1+K_2.

In our model, the Breit-Wheeler process is described by the transition from the initial two-photon state $|K_1K_2\rangle \equiv a(K_1)^\dagger\, a(K_2)^\dagger\, |vac\rangle$ to the final group of electron-positron states $|PQ\rangle \equiv b(P)^\dagger\, d(Q)^\dagger\, |vac\rangle$. For given

photon momenta K_1 and K_2, we will identify the most effectively coupled momenta P and Q in the sections below, which must fulfill the momentum conservation equation $K_1 + K_2 = P + Q$. Due to the assumption that both photons are infinitely extended and therefore constantly interacting, we can derive here a pair-creation rate Γ_{BW} for the Breit-Wheeler pair process, which is identical to the decay rate of the initial state. For simplicity we focus here on those created electrons that propagate into the positive x-direction associated with a positive momentum P and the positron's momentum is always defined as $Q \equiv -P + K_1 + K_2$.

In order to capture the main mechanism for the Breit-Wheeler process, we consider only those interactions that occur in lowest order of the coupling constant λ. As we display in Figure 1, the initial state $|\Psi(t=0)\rangle = |K_1, K_2\rangle$ is coupled via the photon annihilation provided by V_3 (which is proportional to $b^\dagger d^\dagger a$) to two sets of continuum states characterized by an electron-positron pair and a photon with momentum K_1 or K_2.

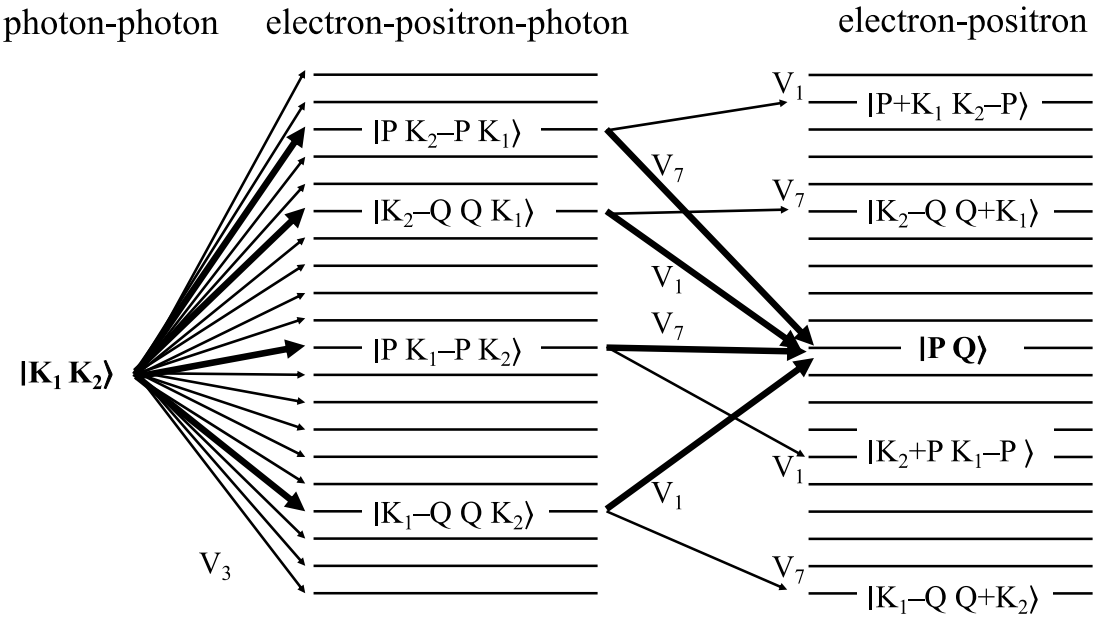

Figure 1 Sketch of the relevant couplings between the initial two-photon state $|K_1K_2\rangle$ and the final electron-positron states $|PQ\rangle$, where $P + Q = K_1 + K_2$. The initial state is coupled to two single-photon continua characterized by K_1 and K_2, respectively. Each state of this continuum is then coupled to exactly two electron-positron states.

Under the continued annihilation of the remaining photon provided by the interactions V_1 ($\propto b^\dagger ba$) or V_7 ($\propto dd^\dagger a$), each (continuum) state is then coupled to two unique pairs of electron-positron states. In this restricted subspace, the time evolution of the state $|\Psi(t)\rangle$ can be expressed by the expansion

$$|\Psi(t)\rangle = C_{\omega_1\omega_2}(t)\,|K_1K_2\rangle + \Sigma_p\, C_{e^-e^+}(p,t)\,|p\ q\rangle + \Sigma_p\, C_{K1}(p,t)\,|p\ q\ K_1\rangle + \Sigma_p\, C_{K2}(p,t)\,|p\ q\ K_2\rangle \qquad (3.1)$$

where the corresponding value for the positron momentum q is different in each state and is fixed by the momentum conservation. The reduction of the dynamically accessible Hilbert space to a restricted subspace containing only states with two photons, two fermions and states with a single photon and two fermions does not permit the simulation of several higher order processes. For example, a subsequent collision of the created electron-positron pair can generate four photon states that were omitted in this approach. Our theoretical framework is therefore intrinsically perturbative in nature and omits some of the processes that could contribute to the radiative corrections.

In Appendix A we derive the equations for these expansion coefficients, that lead to:

$$i\,dC_{\omega_1\omega_2}/dt = (\omega_1+\omega_2)\,C_{\omega_1\omega_2} + \Sigma_p\,\gamma(p,K_2)\,C_{K1}(p) + \Sigma_p\,\gamma(p,K_1)\,C_{K2}(p) \qquad (3.2a)$$

$$i\,dC_{K1}(p)/dt = E_{K1}(p)C_{k1}(p) + \gamma(p,K_2)C_{\omega_1\omega_2} + \kappa(p,K_1)C_{e^-e^+}(p+K_1)$$
$$+ \text{sign}\,[(p-K_1-K_2)(p-K_2)]\,\kappa(p-K_1-K_2,K_1)\,C_{e^-e^+}(p) \qquad (3.2b)$$

$$i\,dC_{K2}(p)/dt = E_{K2}(p)\,C_{k2}(p) + \gamma(p,K_1)\,C_{\omega_1\omega_2} + \kappa(p,K_2)\,C_{e^-e^+}(p+K_2)$$
$$+ \text{sign}\,[(p-K_1-K_2)(p-K_1)]\,\kappa(p-K_1-K_2,K_2)\,C_{e^-e^+}(p) \qquad (3.2c)$$

$$i\,dC_{e^-e^+}(p)/dt = (E_p+E_q)\,C_{e^-e^+}(p)$$
$$+ \text{sign}\,[(p-K_1-K_2)(p-K_2)]\kappa(p-K_1-K_2,K_1)\,C_{K1}(p) + \kappa(p,-K_1)\,C_{K1}(p-K_1)$$
$$+ \text{sign}\,[(p-K_1-K_2)(p-K_1)]\kappa(p-K_1-K_2,K_2)\,C_{K2}(p) + \kappa(p,-K_2)\,C_{K2}(p-K_2) \qquad (3.2d)$$

where coupling functions $\gamma(p,K)$ and $\kappa(p,K)$ are defined in terms of the Γs in Appendix A. Due to hermiticity of the corresponding effective Hamiltonian in this sub-space, this set of equations preserves the total norm of the state, given by $1 = \langle\Psi(t)|\Psi(t)\rangle = |C_{\omega_1\omega_2}(t)|^2 + \Sigma_p\,[|C_{e^-e^+}(p,t)|^2 + |C_{K1}(p,t)|^2 + |C_{K2}(p,t)|^2]$.

4 Simplification of the essential state system to only a single final state

4.1 The six-level system

The equations (3.2) describe the coupling of a single initial state $|K_1,K_2\rangle$ to a set of final electron-positron states $|p,q\rangle$. However, to better understand the role of final state and the corresponding

dynamics, we first focus on the dynamics leading to a particular single electron-positron final state $|P,Q=K_1+K_2-P\rangle$, whose momenta are denoted by capital letters. In other words, we will examine the interaction between the initial and final state and only four other intermediate states with coupling between them indicated by the thick arrows in Figure 1. As illustrated in the figure, only the three operators V_1, V_3 and V_7 in the interaction energy operator can couple the initial two photon state $|K_1,K_2\rangle$ to the final electron-positron state $|P,Q= -P+K_1+K_2\rangle$. Note that the four intermediate states take the general form $|p,q,k\rangle$, describing a single electron-positron pair and one photon. They are the result of the action of V_3 (containing the operator product $b^\dagger d^\dagger a$) onto $|K_1,K_2\rangle$, where the remaining photon is annihilated and converted to an electron-positron pair. For notational simplicity, these intermediate states are abbreviated as

$$|A\rangle \equiv |p=P,\ q= -P+K_1,\ k=K_2\rangle \tag{4.1a}$$

$$|B\rangle \equiv |p=P,\ q= -P+K_2,\ k=K_1\rangle \tag{4.1b}$$

$$|C\rangle \equiv |p= -Q+K_1,\ q=Q,\ k= K_2\rangle \tag{4.1c}$$

$$|D\rangle \equiv |p= -Q+K_2,\ q=Q,\ k= K_1\rangle \tag{4.1d}$$

These four intermediate states have the bare state energies $E_A \equiv \omega_2 + E_P + E_{-P+K1}$, $E_B \equiv \omega_1 + E_P + E_{-P+K2}$, $E_C \equiv \omega_2 + E_{-Q+K1} + E_Q$ and $E_D \equiv \omega_1 + E_{-Q+K2} + E_Q$. Finally, the action of V_1 or V_7 reduces these four states to $|PQ\rangle$. In the following we shorten our notation even more by defining the expansion amplitudes as

$$C_K \equiv C_{\omega_1\omega_2}(K) \tag{4.2a}$$

$$C_A(p) \equiv C_{K2}(p) \tag{4.2b}$$

$$C_B(p) \equiv C_{K1}(p) \tag{4.2c}$$

$$C_C(p) \equiv C_{K2}(p-K_2) \tag{4.2d}$$

$$C_D(p) \equiv C_{K1}(p-K_1) \tag{4.2e}$$

$$C_P \equiv C_{e^-e^+}(p) \tag{4.2f}$$

Equivalently, we come to the same coupling terms, if we had expanded the time evolution operator up to second order in time, (corresponding to the weak-coupling limit), to obtain $\mathrm{Exp}[-i\,H t] \approx 1 - i\,H\,t + (-i\,H\,t)^2/2$.

This truncated propagator couples the initial state solely to the four intermediate states. As any interaction would change the number of photons in any state, the Hamiltonian does not couple the four intermediate states directly to each other. Using the more compact notation, the six time-dependent expansion coefficients have to satisfy

$$i\, dC_K/dt = (\omega_1 + \omega_2)\, C_K + \\ + [\gamma_A(P)\, C_A(P,t) + \gamma_B(P)\, C_B(P,t) + \gamma_C(P)\, C_C(P,t) + \gamma_D(P)\, C_D(P,t)] \quad (4.3a)$$

$$i\, dC_A(P)/dt = E_A(P)\, C_A + \gamma_A(P)\, C_K + \kappa_A(P)\, C_P \quad (4.3b)$$

$$i\, dC_B(P)/dt = E_B(P)\, C_B + \gamma_B(P)\, C_K + \kappa_B(P)\, C_P \quad (4.3c)$$

$$i\, dC_C(P)/dt = E_C(P)\, C_C + \gamma_C(P)\, C_K + \kappa_C(P)\, C_P \quad (4.3d)$$

$$i\, dC_D(P)/dt = E_D(P)\, C_D + \gamma_D(P)\, C_K + \kappa_D(P)\, C_P \quad (4.3e)$$

$$i\, dC_P/dt = (E_p + E_Q)\, C_P + \\ + \kappa_A(P)\, C_A(P,t) + \kappa_B(P)\, C_B(P,t) + \kappa_C(P)\, C_C(P,t) + \kappa_D(P)\, C_D(P,t) \quad (4.3f)$$

These equations are similar to Eqs. (3.2), but do not contain any summations over infinite number of states. The values for the coupling constants follow from the scalar products between the corresponding states. For example, $\gamma_A \equiv \langle A|V_3|K_1K_2\rangle = \langle\, p=P,\, q=-P+K_1,\, k=K_2\, |V_3|\, K_1K_2\rangle = \langle\, p=P,\, q=-P+K_1\, |V_3|\, K_1\rangle = g\, \Gamma_{UD}(P,P-K_1, K_1)$. They are consistent with the γ and κ functions defined in Appendix A. Here is the complete list of the relevant eight couplings

$$\gamma_A(P) = g\, \Gamma_{UD}(P,P-K_1, K_1) \quad (4.4a)$$

$$\gamma_B(P) = g\, \Gamma_{UD}(P,P-K_2, K_2) \quad (4.4b)$$

$$\gamma_C(P) = g\, \Gamma_{UD}(P-K_2,P-K_1-K_2, K_1) \quad (4.4c)$$

$$\gamma_D(P) = g\, \Gamma_{UD}(P-K_1,P-K_1-K_2, K_2) \quad (4.4d)$$

$$\kappa_A(P) = -\, g\, \Gamma_{DD}(P-K_1, P-K_1-K_2, K_2) \quad (4.4e)$$

$$\kappa_B(P) = -\, g\, \Gamma_{DD}(P-K_2, P-K_1-K_2, K_1) \quad (4.4f)$$

$$\kappa_C(P) = g\, \Gamma_{UU}(P, P-K_2, K_2) \quad (4.4g)$$

$$\kappa_D(P) = g\, \Gamma_{UU}(P,P-K_1, K_1) \quad (4.4h)$$

4.2 Reduction to a two-level system via adiabatic elimination of the four intermediate states

4.2.1 Derivation of the set of equations

As the energies of the four intermediate states are sufficiently larger than the bare energies of the initial and final states $|K_1K_2\rangle$ and $|PQ\rangle$, we can adiabatically eliminate these non-resonant intermediate states. To do so, we transform all first six amplitudes for each momentum P into a rotating coordinate system, $C_j \equiv \exp[-i(\omega_1 + \omega_2)t]\, c_j$ (for j=K, A, B, C, D, P). In order to eliminate the four coefficients associated with the intermediate states, we approximate $d/dt\, c_j(P) = 0$ for j=A, B, C and D. This allows us to solve the resulting algebraic equations for the four c_j. If we insert the c_j into the equation for c_K and c_P and transform back to the original (not-rotated) coordinate frame, we obtain a two-level like system [29,30]:

$$i\, dC_K/dt = (\omega_1 + \omega_2 + \alpha_1)\, C_K + \Omega(P)\, C_P \tag{4.5a}$$

$$i\, dC_P/dt = \Omega(P)\, C_K + [E_P + E_Q + \alpha_2(P)]\, C_P \tag{4.5b}$$

where the initial two-photon amplitude C_K is coupled directly to the final state amplitude C_P. Here the effective coupling Ω and energy shifts α_1 and α_2 are given by

$$\alpha_1(P) \equiv \gamma_A(P)^2\, (\omega_1+\omega_2-E_A(P))^{-1} + \gamma_B(P)^2\, (\omega_1+\omega_2-E_B(P))^{-1} + \gamma_C(P)^2\, (\omega_1+\omega_2-E_C(P))^{-1} + \gamma_D(P)^2\, (\omega_1+\omega_2-E_D(P))^{-1} \tag{4.6a}$$

$$\alpha_2(P) \equiv \kappa_A(P)^2\, [\omega_1+\omega_2-E_A(P)]^{-1} + \kappa_B(P)^2\, [\omega_1+\omega_2-E_B(P)]^{-1} + \kappa_C(P)^2\, [\omega_1+\omega_2-E_C(P)]^{-1} + \kappa_D(P)^2\, [\omega_1+\omega_2-E_D(P)]^{-1} \tag{4.6b}$$

$$\Omega(P) \equiv \gamma_A(P)\, \kappa_A(P)\, [\omega_1+\omega_2-E_A(P)]^{-1} + \gamma_B(P)\, \kappa_B(P)\, [\omega_1+\omega_2-E_B(P)]^{-1} + \gamma_C(P)\, \kappa_C(P)\, [\omega_1+\omega_2-E_C(P)]^{-1} + \gamma_D(P)\, \kappa_D(P)\, [\omega_1+\omega_2-E_D(P)]^{-1} \tag{4.6c}$$

Before we analyze the Breit-Wheeler process from a space-time resolved scattering perspective in Section 6, we examine the dynamics for the case where the initial state $|K_1K_2\rangle$ is coupled to only a single final state $|PQ\rangle$. This has three purposes. First, we will test the validity of the adiabatic elimination of the four intermediate states. Second, it will provide approximate but analytical solution for an easier analysis of the spatially resolved scattering. Third, it permits us to derive the Breit-Wheeler rate Γ_{BW} based on the Fermi-Golden rule approach.

4.2.2 Range of validity of the adiabatic elimination of the intermediate states

For the special case where the initial state $|K_1K_2\rangle$ is coupled to only a single final state $|PQ\rangle$, the corresponding effective Hamiltonian 2×2 matrix is given by $\{\{\omega_1 + \omega_2 + \alpha_1(P), \Omega(P)\},\{\Omega(P), E_P + E_Q + \alpha_2(P)\}\}$. The Hamiltonian has the two eigen-energies $\Sigma E/2 \pm \gamma/2$, where $\gamma \equiv [\Delta E^2 + 4\,\Omega^2]^{1/2}$ and where the difference and the sum of the diagonal elements are abbreviated as $\Delta E \equiv \omega_2+\omega_1+\alpha_1-E_P-E_Q-\alpha_2$ and $\Sigma E \equiv \omega_2+\omega_1+\alpha_1+E_P+E_Q+\alpha_2$. We note that even if the two bare energies $\omega_1+\omega_2$ and E_P+E_Q were chosen equal to each other and $\alpha_1=\alpha_2=0$, the coupling Ω would lift any energy degeneracy, as γ is always non-zero. Due to the occurrence of avoided crossings, it is not even possible to choose any set of bare energies such that the spectrum becomes degenerate.

With the initial conditions $C_K(t=0) = 1$ and $C_P(t=0) = 0$, this set of two coupled equations can be easily solved analytically and we obtain the following solution for the two amplitudes and the corresponding probabilities

$$C_K(t) = \left[\mathrm{Cos}(\gamma\, t/2) - i\,\Delta E\,\mathrm{Sin}[\gamma\, t/2]/\gamma\right]\mathrm{Exp}[-i\,\Sigma E\, t/2] \qquad (4.7a)$$

$$C_P(t) = -2\,i\,\Omega\,\mathrm{Sin}[\gamma\, t/2]/\gamma\;\mathrm{Exp}[-i\,\Sigma E\, t/2] \qquad (4.7b)$$

$$|C_K(t)|^2 = \mathrm{Cos}^2(\gamma\, t/2) + \Delta E^2/\gamma^2\;\mathrm{Sin}^2[\gamma\, t/2] \qquad (4.7c)$$

$$|C_P(t)|^2 = 4\,\Omega^2\,\mathrm{Sin}^2[\gamma\, t/2]/\gamma^2 \qquad (4.7d)$$

In the special case $\Omega = 0$ it reduces to $C_K(t) = \mathrm{Exp}[-i(\omega_1+\omega_2+\alpha_1)\, t]$ and $C_P(t) = 0$, as expected. The period of this population transfer is given by $2\pi/\gamma$, which in the small coupling limit and for $\Delta E=0$ becomes π/Ω. We can also read off the maximum population transfer into the state $|PQ\rangle$, associated with the characteristic time $t^* \equiv \pi/\gamma$, as

$$\max\left|\langle PQ|\Psi(t)\rangle\right|^2 = |C_2(t^*)|^2 = 4\,\Omega^2/(\Delta E^2 + 4\,\Omega^2] \qquad (4.8)$$

This means, the largest pair-creation probability for the Breit-Wheeler process $[|C_P(t^*)|^2 =1]$ is possible if the "dressed" resonance condition $\omega_1 + \omega_2 + \alpha_1 = E_P + E_Q + \alpha_2$, i.e. $\Delta E=0$, is fulfilled. Interestingly, as α_1 and α_2 are not identical to each other, the naïve resonance condition based on the bare energies, i.e., $\omega_1 + \omega_2 = E_P + E_Q$

becomes less meaningful. For example, if we take the state space with $P_{tot} = 0$, then $\Delta E=0$ can be solved for P as a function of K, leading to $E_P = \omega_1 + (\alpha_1 - \alpha_2)/2$. As the bare energies of the four intermediate states are larger than $\omega_1 + \omega_2$, both energy shifts α_1 and α_2 are negative. Whether the true fermionic "resonance" energy that maximizes the created particle yield needs to be larger or smaller than the photon's bare energy depends on the relative magnitudes of the coupling constants γ and κ. This dependence on K_1 might also be in contradiction to prior claims [1] that it is "unnecessary to use quantized light wave in the pair creation problem".

In order to estimate the validity of the adiabatic elimination of the four intermediate levels, we need to choose some specific parameters. In our numerical illustrations we use atomic units where the speed of light is c=137.036 a.u. The choice of the bare masses M=1 a.u. and m = 0.1 a.u., requires the photon momenta to be at least $K_1 = -K_2 = 136.35$ a.u. to create an electron-positron pair at rest, corresponding to the energy $2\omega_1$. For the photon momentum, we chose from now on $K_1 = 150$ a.u. and $K_2 = -150$ a.u., such that $Q = -P$ to preserve the total momentum.

In the very weak coupling limit, one could (incorrectly) expect that the energy shifts α_1 and α_2 can be neglected. Here the bare-energy resonance condition $2\omega_1 = E_P + E_Q$ would predict $P_{bare} = 62.52$ a.u.. However, in this bare-energy degenerate case the relevant energy shift simplifies to $\Delta E = \alpha_1 - \alpha_2$, which scales quadratically in λ and therefore has the same scaling as Ω. Therefore, the maximum amplitude of the upper state, given by $\max[|C_P|^2] = 4\,\Omega_2/\gamma_2 = 4\,\Omega_2\,[\Delta E_2 + 4\,\Omega_2]^{-1}$, does not approach unity, but a λ-independent value equal to $\max[|C_P|^2] = 4\,\Omega_2\,[(\alpha_1-\alpha_2)^2 + 4\,\Omega_2]^{-1} = 0.2488$ for $P = P_{bare}$. This means that even in the very weak perturbative limit, the resonant value of P_{res}, that satisfies $\Delta E = 0$, can never be chosen equal to P_{bare} to maximize $|C_P(t)|^2$, even though P_{res} certainly approaches P_{bare} in the small λ-limit. In fact, the largest population becomes extremely sensitive to the particular choice of P. For example, for $\lambda = 0.1$, we obtain $\max[|C_P|^2] = 1$ for $P = P_{res} = 62.52139651917575$, but only $\max[|C_P|^2] = 0.2488$ for $P = P_{bare} = 62.52138319775083$.

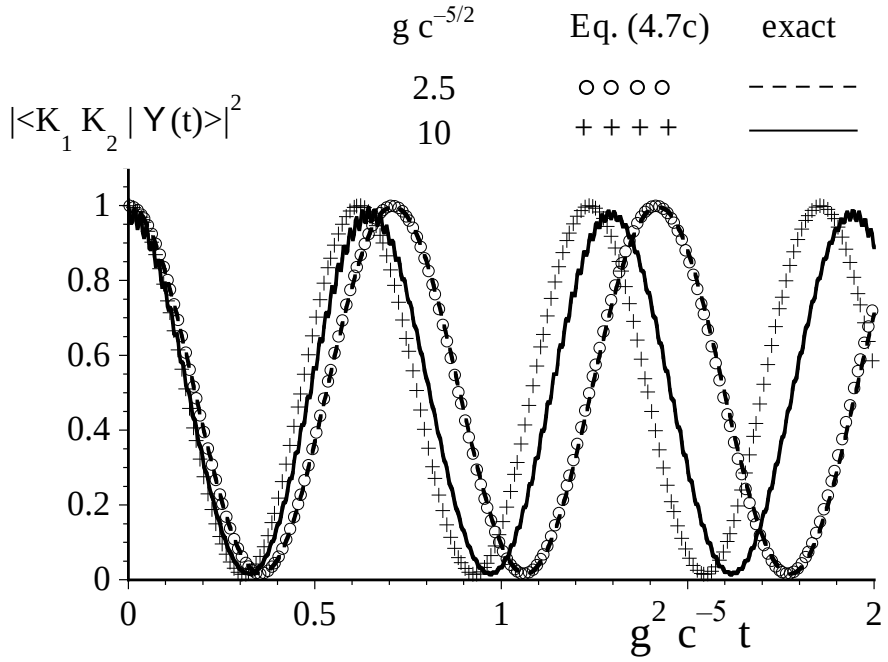

Figure 2 Range of validity of the adiabatic elimination of the four intermediate states $|A\rangle$, $|B\rangle$, $|C\rangle$ and $|D\rangle$. We compare the exact time dependence of the two-photon probablity $|C_1(t)|^2 = \langle K_1K_2|\Psi(t)\rangle|^2$ based on the coupling to the electron-positron state $|PQ\rangle$ via the four intermediate states with the analytical but approximate solution given by Eq. (4.7c) for $g = 2.5\ c_{2/5}$ (circles) and $g = 10\ c_{2/5}$ (crosses). [$K_1 = 150$ a.u., $K_2 = -K_1$, fermion mass $M = 1$ a.u., boson mass $m = 0.1$ a.u., in order to stay on resonance ($\Delta E = 0$, such that $\max |C_2(t)|^2 = 1$), we chose $P = 63.33266228629012$ (for $g = 2.5\ c_{2/5}$) and $P = 74.8682167011005$ (for $g = 10\ c_{2/5}$).

We found that for g less than $2.5c_{5/2}$, the first five oscillations in $|C_K(t)|^2$ predicted by the approximate analytical expression Eq. (4.7c) were graphically indistinguishable from the exact solutions that contained the four intermediate states. In order to show how the higher-order corrections manifest themselves in the time-dependence of $|C_K(t)|^2$ we compare in Figure 2 the exact behavior for $g = 2.5\ c_{5/2}$ (continuous line) and $g = 10\ c_{5/2}$ (dashed line) with the predicted behavior according to Eq. (4.7c). In order to stay at full resonance ($\Delta E = 0$), such that $\max[|C_P|^2] = 1$, we had to increase P as the coupling g was increased. As $\Omega(P)$ itself increases with P in this domain (see Figure 4a of Section 5.2.1 below), even the scaled frequency $\gamma/g^2 = [\Delta E^2 + 4\,\Omega^2]^{1/2}/\,g^2$ increases with g.

The correction to $|C_K(t)|^2$ due to the presence of the intermediate states manifests itself in two ways. First, the actual oscillation period is longer than the predicted value $\pi/\gamma = \pi/[(\alpha_1 - \alpha_2)^2 + 4\,\Omega^2]$ such that after a few oscillations the true graph gets out of phase with the approximate one predicted by Eq. (4.7c). Second, the graph is no longer sinusoidal, but there are additional larger frequencies contained in the graph that reflect the

large energy difference between the initial and the four intermediate states.

5. Dynamics of a single two-photon state coupled to an infinite set of final states

5.1 The model equations

In this Section we will lift the restriction that the initial two-photon state is coupled only to a single final electron-positron state with a specific momentum P and Q with $P + Q = K_1 + K_2$. This situation was also depicted by the couplings in Fig. 1, where the initial state $|K_1K_2\rangle$ is coupled via the intermediary three-particle states to an entire set of final states $|PQ\rangle$. In other words, we assume here that our state is given by the superposition $|\Psi(t)\rangle = C_K(t)\,|K_1K_2\rangle + \Sigma_P\, C_P(t)\,|P\,Q\rangle$, with the norm given by $1 = \langle\Psi(t)|\Psi(t)\rangle = |C_K(t)|^2 + \Sigma_P\, |C_P(t)|^2$. Furthermore, if we remove the energy shifts α_1 and $\alpha_2(P)$ (that arose from the adiabatic elimination) from Eqs. (4.5), we obtain

$$i\, dC_K/dt = (\omega_1 + \omega_2)\, C_K + \Sigma_P\, \Omega(P)\, C_P \tag{5.1a}$$

$$i\, dC_P/dt = (E_P + E_Q)\, C_P + \Omega(P)\, C_K \tag{5.1b}$$

In order to avoid any charge or mass renormalization at this stage, we have formally set the two energy shifts α_1 and α_2 equal to zero. A more systematic and mathematically rigorous derivation of this "renormalization" is beyond the goal of this work, so we postpone the discussion of this rather nontrivial issue to further work and just quote a few prior works that have examined various renormalization schemes [31-34] for general approaches that are similar to this work.

This set of equations serves as the main model for this section. We should point out that the dynamics will depend on the choice of the set of final momenta. While the time evolution of $C_K(t)$ should not depend on the choice of the largest momentum P (if chosen sufficiently large), we would expect that the average mode spacing Δp between the resonantly excited momentum states $|P\,Q\rangle$, will affect the decay rate of the amplitude $C_K(t)$. It should be obvious that this rate should therefore increase with an increasing density of the final states, which is proportional to Δp^{-1}. As we will argue below, this Δp dependence is actually quite physical and expected. Also, to simply replace the summation in Eq. (5.1a) $\Sigma_P\, \Omega(P)\, C_P$ by the integral $\int dP\, \Omega(P)\, C_P$ would be unphysical as this would violate the dimension of the equation, as the amplitudes and C_K and C_P are unitless.

5.2 Time dependence of the solutions $C_K(t)$ and $C_P(t)$

The set of coupled equations for C_K and the set of C_P can be solved analytically using the dominant pole approximation. As this type of coupled equations is rather standard in atomic physics, we shift the solution technique based on Laplace-transformations and Green's function-based to Appendix B. In the time domain the final solutions are

$$C_K(t) = \mathrm{Exp}[-i(\omega_1+\omega_2-\chi)t]\,\mathrm{Exp}[-\Gamma_{BW}\,t/2] \tag{5.2a}$$

$$C_P(t) = -\Omega(P)\,\mathrm{Exp}[-i(E_P+E_Q)t]\,\big[\mathrm{Exp}[i(\Delta E+i\,\Gamma_{BW}/2)\,t]-1\big]/(\Delta E+i\,\Gamma_{BW}/2) \tag{5.2b}$$

$$|C_K(t)|^2 = \mathrm{Exp}[-\Gamma_{BW}\,t] \tag{5.2c}$$

$$|C_P(t)|^2 = \Omega(P)^2/[\Delta E^2+(\Gamma_{BW}/2)^2]\,\big[1+\mathrm{Exp}[-\Gamma_{BW}\,t]-2\,\mathrm{Exp}[-\Gamma_{BW}/2\,t]\,\mathrm{Cos}[\Delta E t]\big] \tag{5.2d}$$

where we have defined the energy difference $\Delta E = (E_P+E_Q)-(\omega_1+\omega_2)+\chi$ and χ denotes the principal part of the integral $\int dP\;\Omega(P)^2/[(\omega_1+\omega_2)-(E_P+E_Q)]$. The parameter

$$\Gamma_{BW} \equiv 2\pi\,[\rho(P_{res,1})\,\Omega(P_{res,1})^2+\rho(P_{res,2})\,\Omega(P_{res,2})^2]/\Delta p \tag{5.3}$$

denotes the Breit-Wheeler pair-creation rate, and the two resonant momenta $P_{res,1}$ and $P_{res,2}$ follow (in the absence of the shift χ) from the solution to the equation $(\omega_1+\omega_2)-(E_P+E_Q)=0$. The density is given by $\rho(P) = \{d[E_P+E_Q]/dP\}_{-1} = c_{-2}\,\{p/E_P - Q/E_Q\}_{-1}$ leading to

$$\rho(P) = c_{-2}\,\{p\,[M^2c^4+c^2P^2]_{-1/2}-(P_{tot}-P)\,[M^2c^4+c^2(P_{tot}-P)^2]_{-1/2}\}_{-1}. \tag{5.4}$$

The dependence of the electron-positron pair creation rate Γ_{BW} on the numerical parameter such as the mode spacing Δp is physically fully expected. If we return to the original (unitless) coupling constant λ, $(=g\,c_{-5/2}\Delta p_{-1/2})$, we see that the scaling $\Gamma_{BW} \sim \lambda^4\,\Delta p$ corresponds to a meaningful inverse proportionality to the physical extension L of our numerical box $(L=2\pi/\Delta p)$, i.e. $\Gamma_{BW} \sim L_{-1}$. This conclusion is fully consistent with the corresponding quantum mechanical wave-based and also quantum particle-based picture of two colliding photons. In the first picture, the corresponding wave function of each photon (with sharp momentum) is normalized to unity, i.e. $\int_{0L} dx\,|\phi(x)|^2 = 1$, which means that the spatial probability density of

each photon is 1/L. The total interaction probability per time unit, Γ_{BW}, is then given by the product of the two spatial probabilities integrated over the total interaction length L, resulting in the expected overall 1/L dependence. Very similarly, if we assume that the two photons were spatially localized at different locations with the box L and need to overlap in order to annihilate (into the fermionic particle pair), then the average delay time for this collision to happen ($\sim\Gamma_{BW}^{-1}$) would be linearly proportional to the average distance they have to travel until they meet. As the finite width of each photon can be safely assumed to be independent of L, this distance is directly proportional to L, which suggests again that $\Gamma_{BW} \sim L^{-1}$.

We should point out that the different short-time scaling of $|C_K(t)|^2 = 1 - \Gamma_{BW}\, t$ and $|C_P(t)|^2 = \Omega(P)^2\, t^2$ is not necessarily a contradiction to the normalization $|C_K(t)|^2 + \Sigma_P\, |C_P(t)|^2 = 1$. In fact, while each individual probability grows $|C_P(t)|^2$ *quadratically* in time, it can be shown that the sum $\Sigma_P\, |C_P(t)|^2 = \Gamma_{BW}\, t$ grows only *linearly* in time. We show in Appendix C, that the usual Fermi-Golden rule [35] approach can predict only the short-time decay according to $|C_K(t)|^2 = 1 - \Gamma_{BW}\, t$, however, consistently with the same rate Γ_{BW} as given in Eq. (5.3).

5.3 Range of validity of the Breit-Wheeler decay rate Γ_{BW}

As we have seen in Sec. 4.2.2 for $K_1 = 150$, the adiabatic elimination was justified as long as the coupling constant g was less than about $2.5\, c_{5/2}$. In this section we will examine numerically, for which range of coupling constants g the dominant-pole approximation can be justified, that led to the prediction of an exponential decay, i.e., $|C_K(t)|^2 = \mathrm{Exp}(-\Gamma_{BW}\, t)$.

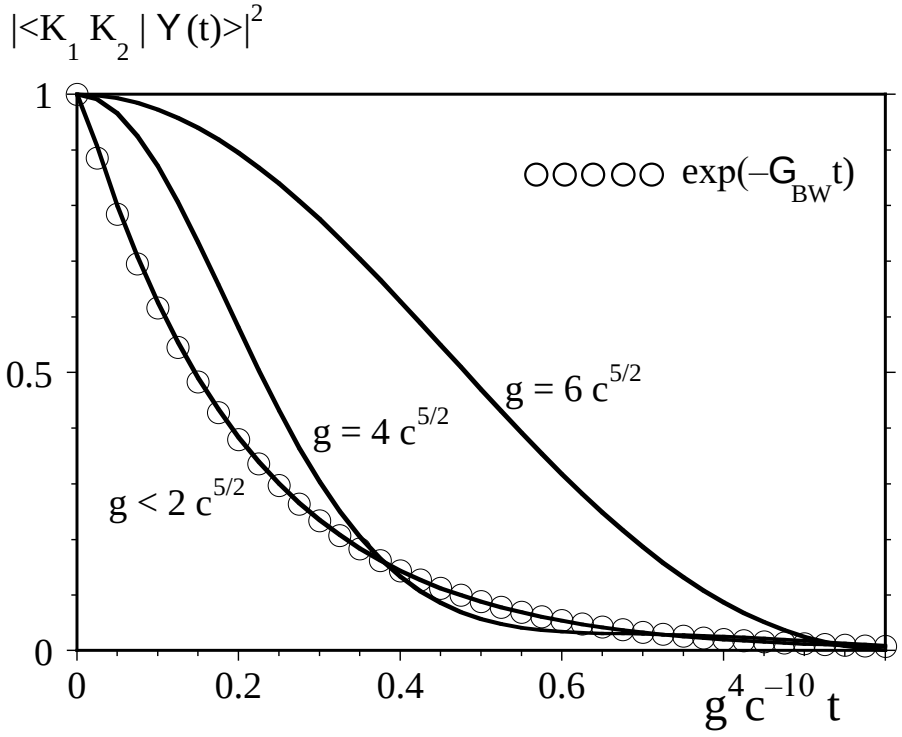

Figure 3 Testing the validity of the dominant-pole approximation. We compare the exact time dependence of $|C_K(t)|^2 = \langle K_1 K_2|\Psi(t)\rangle|^2$ with the approximate exponential decay $\mathrm{Exp}[-\Gamma_{BW} t]$ (open circles). [$K_1 = 150$ a.u., $K_2 = -K_1$, fermion mass M =1 a.u., boson mass m = 0.1 a.u., number of final states $|PQ\rangle$ was 800 with $\Delta p = 2\pi/L$ and L = 16 a.u.]

In order to obtain the exact numerical solutions to the full set of equations (5.1), we have discretized the momentum P on a N-dimensional grid (i.e. $P_n = (-N/2 + n)\,\Delta p$, n = 1,2,... N), and solved the resulting (1+N) coupled equations numerically. We have increased the number of grid points N until we obtained numerically converged results.

In Figure 3 we compare the exact decay of $|C_K(t)|^2$ obtained from the numerical solution to the coupled set of equations (5.1) with the analytical prediction given by Eq. (5.2c) (open circles). We found that for $K_1 = 150$ a.u. and $\Delta p = 1$ the numerical value of the Breit-Wheeler decay rate computed for $P_{res} = P_{bare}$ is given by $\Gamma_{BW} \approx \lambda_4\, 1.9$. We see that for $g < 2\, c_{5/2}$ the agreement is superb, whereas for a larger g, such as $g = 4\, c_{5/2}$ the deviation is obvious. For an even larger coupling we see that the analytical expression becomes very inaccurate, as the coupling to the other states is so large, that we even observe a non-exponential decay.

As a side issue, we remark that there is also an effect due to the discreteness of the final momentum states, characterized by a non-zero mode spacing $\Delta p = 2\pi/L$. For example, had we repeated the calculation in Figure 3 with a larger Δp, then the perfect match with the exponential decay would only occur for times $t < L/c$, corresponding to the minimum time it takes for a particle with speed c to cover the distance L. For $t > L/c$ the system is able to resolve the underlying discreteness of the energies and the probability $|C_K(t)|^2$ would reveal a quasi-oscillatory behavior, with periods that depend on Δp.

We should note that for small g the range of dynamically accessible momentum states $|PQ\rangle$ is much narrower than the coupling provided by $\Omega(P)$, which we have graphed in Figure 4a. It takes a maximum at around $P \approx \pm 160$ a.u. In Figure 4b we graph the actual final momentum distribution of the created positrons, given by the numerically obtained $|C_P(t)|^2$, together with its approximate but analytical prediction from Eq. (5.2d) and given by $|C_P(t\rightarrow\infty)|^2 = \Omega(P)^2/[\Delta E^2 + (\Gamma_{BW}/2)^2]$. For small values of g the actual momentum distribution $|C_P(t)|^2$ is centered around $P \approx \pm 62.52$ a.u., close to P_{bare} as expected in this limit. The agreement between the exact and the analytical estimate is very good. As we increase g, the estimated distribution widens significantly but remains centered close to P_{bare}. While the true distribution $|C_P(t)|^2$ has a qualitatively similar shape, its maximum has shifted to smaller momenta, reflecting higher-order corrections that are neglected by the solutions of Eq. (5.2d).

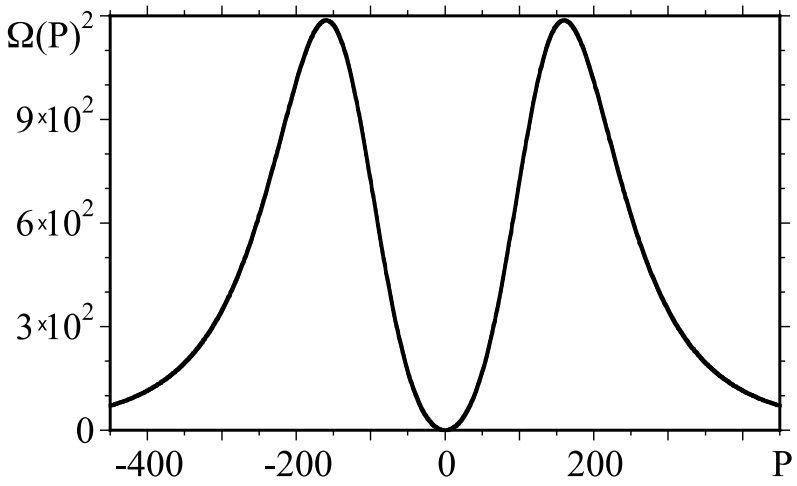
Ω(P)2
9×102
6×102
3×102
0
-400
-200
0
200
P

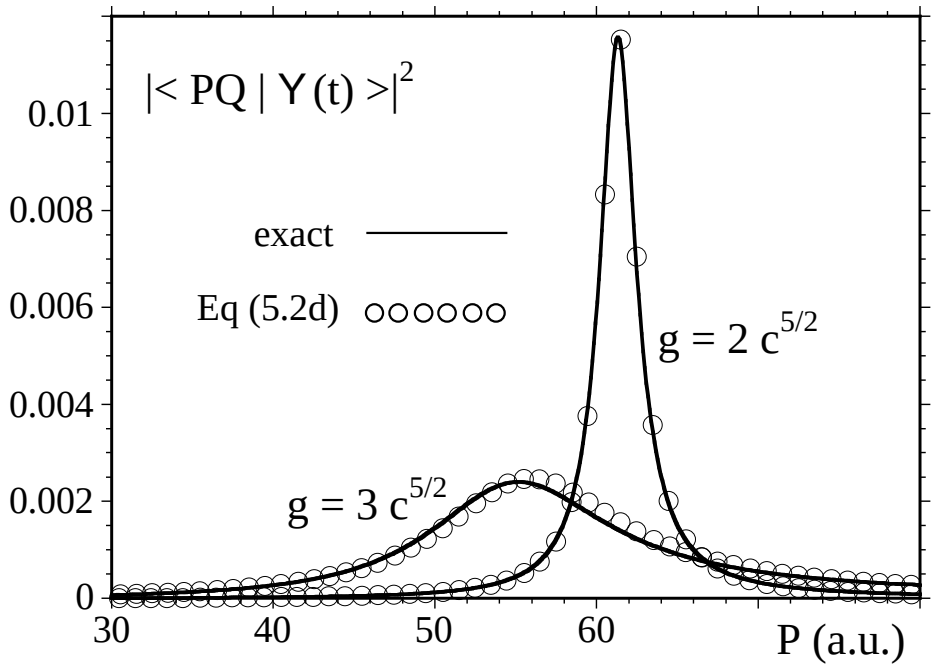

Figure 4 (a) The effective coupling function $\Omega(P)^2$ for $g = 2\ c^{5/2}$ and $\Delta p = 2\pi/4$. (b) The final momentum distribution of the created bare electron/positron pairs given by $|C_P(t)|^2 = |\langle PQ|\Psi(t)\rangle|^2$ at time t = 0.078 a.u. for $g = 2\ c^{5/2}$ and at time t = 0.0154 a.u. for $g = 3\ c^{5/2}$. For comparison, we also include by the circles the (normalized) Lorentz-like distribution $\Omega^2/[\Delta E^2+(\Gamma_{BW}/2)^2]$ according to Eq. (5.2d). These distributions were shifted to smaller momenta by 1.2 (7.4) for $g = 2\ c^{5/2}$ ($3\ c^{5/2}$) to match the exact data. We chose $\Delta p=2\pi/64$ with 2400 momentum states. [The other parameters are fermion mass M=1 a.u., boson mass m=0.1 a.u., K_1=150, K_2=– K_1]

Finally, we should remark that the narrowing of the distribution $\Omega(P)^2/[\Delta E^2 + (\Gamma_{BW}/2)^2]$ with decreasing g is not so unexpected in view of the different scaling behavior of the energy difference ΔE and Γ_{BW} with g. In the limit of extremely small g, we obtain $|C_P(t\rightarrow\infty)|^2 = \Omega(P)^2/\Delta E^2$, which is even singular at the resonance, permitting us to restrict the dynamically relevant final states to only two very narrow bands centered around the momentum $\pm P_{bare}$. While the dynamics of $|C_K(t)|^2$ remains an exponential decay in this limit with a decay rate Γ_{BW}, i.e. $|C_K(t)|^2 \approx 1 - 2\pi\ \rho(E)\ \Omega^2/\Delta p\ t$, the model based on only a single discrete final state (see Section 4.2.2 above) predicted a different short-time decay, given by $|C_K(t)|^2 = 1 - \Omega^2\ t^2$.

5.4 Discussion of the Breit-Wheeler decay rate

The decay rate Γ_{BW} of the initial two-photon state $|K_1,K_2\rangle$ to a set of final electron-positron states $|P,Q\rangle$ was derived above as $\Gamma_{BW} \equiv 2\pi\,[\rho(P_{res,1})\,\Omega(P_{res,1})^2 + \rho(P_{res,2})\,\Omega(P_{res,2})^2\,]/\Delta p$. We note that this number depends solely on K_1, K_2, g and Δp. As the total momentum $P_{tot} = K_1+K_2$ is conserved, we can also write the decay rate as $\Gamma_{BW} = \Gamma_{BW}(K_1,P_{tot},g,\Delta p)$. As Γ_{BW} was obtained perturbatively it depends on the fourth power of the coupling constant g. However, its dependence on K_1 and K_2 is non-trivial and needs to be studied numerically. In order to examine if there is an incoming photon momentum for which the electron-positron conversion rate is largest, we have graphed in Figure 5 the scaled Breit-Wheeler rate $g^{-4}\,\Gamma_{BW}$ as a function of K_1 for several total momenta P_{tot}.

Note that the threshold value for a photon with momentum K_1 to trigger a pair of electron (with momentum p) and positron (with momentum $P_{tot} - p$) seems to satisfy the (bare) energy conservation condition $\sqrt{(m^2c^4+ K_1^2c^2)} + \sqrt{[m^2c^4+ (P_{tot}-K_1)^2c^2)]} = \sqrt{(M^2c^4+ p^2c^2)} +\sqrt{[(M^2c^4+ (P_{tot}-p)^2c^2)]}$. The threshold values $K_{1\pm}$ are obtained when electron and positron have the same momentum, i.e., when $p = P_{tot}/2$. The thresholds are given by $K_{1\pm} = P_{tot}/2 \pm \sqrt{[\,(M^2-m^2)(P_{tot}^2 + 4M^2c^2)\,]}\,/(2M)$. Only photons with momentum $K_1<K_{1-}$ or $K_1 > K_{1+}$ are able to produce electron-positron pairs. According to these conditions, we can calculate: $K_{1\pm}(P_{tot}=0) = \pm 136.35$, $K_{1-}(P_{tot}=300) = -52.15$, $K_{1+}(P_{tot}=300) = 352.15$, $K_{1-}(P_{tot}=600) = -28.16$, and $K_{1+}(P_{tot}=600) = 628.16$, with $K_{1+} + K_{1-} = P_{tot}$. These estimated $K_{1\pm}$ values are in excellent agreement with the actual threshold values found in the numerical computations displayed in Figure 5.

The important maxima of the Breit-Wheeler rate $g^{-4}\,\Gamma_{BW}$ for $P_{tot}=0$ in Figure 5 can be read off the graphs. For $P_{tot}=0$ we used $P_{res} = \pm\,[(m^2-M^2)\,c^2 + K_1^2)]^{1/2}$ in Eq. (5.3) and found for the optimum momentum for pair-creation $K_{1,0} = \pm 167$. For $P_{tot}\neq 0$, the expressions for P_{res} are more involved, with $P_{res} = P_{tot}/2 \pm 1/(m)\sqrt{\{2c^2m^2\,(m^2-M^2) + 2(m^2-M^2)\sqrt{(K_1^2+c^2m^2)}\,\sqrt{[(K_1-P_{tot})^2+c^2m^2]} + 2K_1^2(m^2+M^2) - 2K_1(m^2+M^2)P_{tot} + m^2P_{tot}^2\}}$. For $P_{tot} = 300$, the optimum momenta are read off at $K_{1,300} = -74$ and 374 and for $P_{tot} = 600$, the peaks are found at $K_{1,600} = -43$ and 643. As discussed more below, the values for $K_{1,300}$ or $K_{1,600}$ can also be derived from the optimum value in the cm-frame $K_{1,0}$ via a Lorentz transformation.

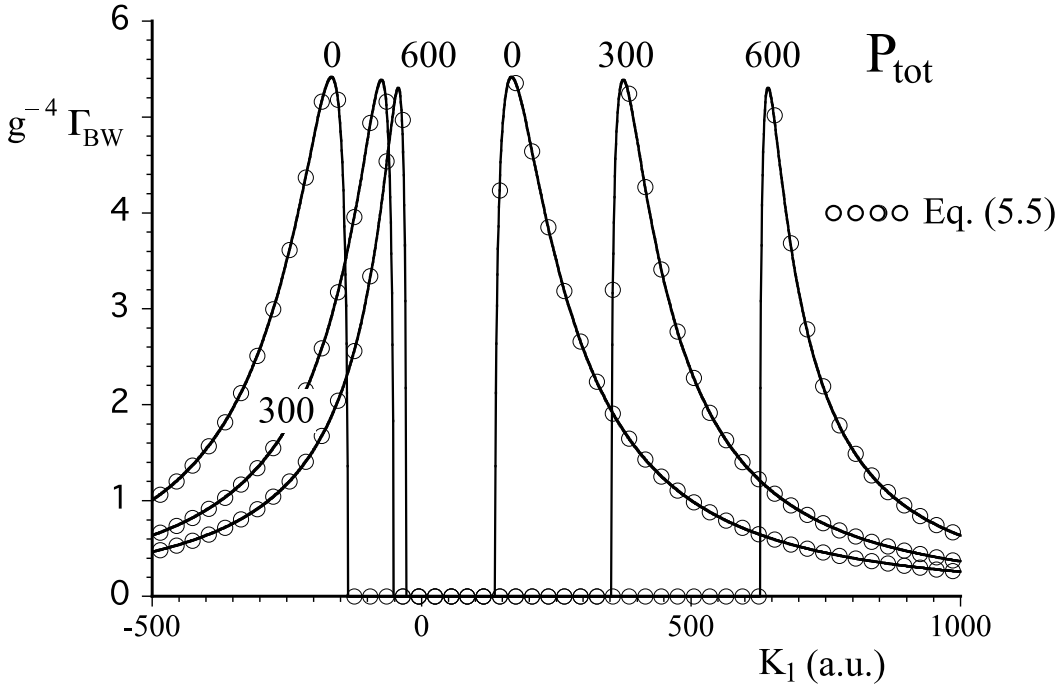

Figure 5 The Breit-Wheeler decay rate Γ_{BW} as a function of the momentum of the incoming photon K_1 and L=16 for the four different total momenta. The circles represent the approximate prediction from Eq. (5.5) based on the Lorentz transformation.

Alternatively, we can also obtain a very similar expression if we assume that the adiabatic elimination of the intermediate states did not violate the Lorentz invariance. Here we can derive the decay rates for $P_{tot} \neq 0$ from the special case of the center-of mass (cm) system, where the total momentum vanishes, i.e., $\Gamma_{BW}(K_1, P_{tot}=0, g, \Delta p)$. In order to construct this, we can find the corresponding Lorentz velocity V, that transforms our system with K_1 and K_2 into the cm system with $P_{tot} = 0$. This leads to the velocity of the moving frame given by $V(K_1, K_2) = c_2\,(K_1+K_2)/[(\omega(K_1) + \omega(K_2)]$. The resulting momentum of the first photon in this frame can be calculated via the usual Lorentz transformation, $K'_1 = [1-(V/c)_2]_{-1/2}\,[K_1 - V\,\omega(K_1)/c_2]$. As the mode spacing $\Delta p = 2p/L$ also needs to be Lorentz transformed $\Delta p = 2\pi/L \rightarrow 2\pi/L'$, where $L' = L\,[1-(V/c)_2]_{1/2}$. We finally obtain,

$$\Gamma_{BW}(K_1, P_{tot}, g, \Delta p) \approx [1 - (V/c)^2]^{1/2}\, \Gamma_{BW}(K'_1, P_{tot}=0, g', \Delta p') \qquad (5.5)$$

Here the inverse of the Lorentz time dilation pre-factor was included based on the (questionable) assumption that we can describe a process at a single location at space. As the coupling constant was defined as a function of Δp as $g \equiv \lambda\, \Delta p^{1/2}\, c^{5/2}$, with the original coupling λ, we have $g' = [1 - (V/c)^2]^{-1/4}\, g$. As a result, the right-hand side of Eq. (5.5) simplifies to $[1 - (V/c)^2]^{1/2}\, \Gamma_{BW}(K'_1, P_{tot}=0, [1 - (V/c)^2]^{-1/4}\, g, \Delta p[1 - (V/c)^2]^{-1/2})$. Due to the quartic scaling of Γ_{BW} with g (or equivalently λ), the Lorentz gamma factor on the front cancels out with those associated with g' and $\Delta p'$.

We should mention that in order to obtain the qualitative match between $\Gamma_{BW}(K_1, P_{tot}, g, \Delta p)$ and $[1-(V/c)^2]^{1/2}\, \Gamma_{BW}(K'_1, P_{tot}=0, g', \Delta p')$, we had to assume that the rate was inversely proportional to the mode spacing Δp, but the coupling constant g had to be changed as well in the moving frame. As we had mentioned in Sec. 2, this constant g was introduced solely for notational convenience from the original coupling constant λ as $g \equiv \lambda\, \Delta p^{1/2}\, c^{5/2}$, which would suggest that λ should not be scaled with Δp. $\Gamma_{BW}(K_1, P_{tot}, \lambda, \Delta p) \approx [1-(V/c)^2]^{1/2}\, \Gamma_{BW}(K'_1, P_{tot}=0, \lambda, \Delta p')$.

In Figure 5 we have included the predictions for $\Gamma_{BW}(K_1, P_{tot}, g, \Delta p)$ based on the assumption of the validity of the Lorentz transform. The circles from Eq. (5.5) match the exact data well, which qualitatively confirms the conjecture that the approximation based on the adiabatic elimination of the intermediaries seems not to violate the invariance.

While the graphical representation of the data seems to suggest a qualitative confirmation of Eq. (5.5), a closer examination reveals a peculiar feature that is presently not fully understood. We will demonstrate this for a concrete numerical example. For $g = 2\, c^{5/2}$, $\Delta p = 2\pi/16$ and $K_1 = -K_2 = 150$, the bare energy resonance condition leads to $P_{res,1} = \pm 62.5213832$ and $\Gamma_{BW} = 77.6007215$. If we transform into a moving frame with velocity V = 10 a.u., (corresponding to the gamma factor $[1-(V/c)^2]^{-1/2} = 1.00267325$), the Lorentz transformed momenta are $K_1' = 139.379992$ and $K_2' = -161.421983$, leading to $P_{res,1} = 51.6675226$ and $P_{res,2} = -73.7095143$. For these four numerical values of the momentum, we obtain $\Gamma_{BW}' = 77.597283$, which differs by only about 0.004 % from the original value. We also note that the two resonant fermion momenta $P'_{res,i}$ obtained from the resonance condition in the moving frame, i.e. $\omega(K_1') + \omega(K_1') = E(P'_{res}) + E(K_1' + K_2' - P'_{res})$, differ from the simple Lorentz transformed momenta, i.e. $[1-(V/c)^2]^{-1/2}\, (P_{res,i} - V\, E(P_{res,i})/c^2]$.

However, if we transform into a more rapidly moving frame with V=130 (corresponding to a gamma

factor 3.16145388, K_1' =22.4748929, K_2' = – 925.961272, $P_{res,1}$ = –254.08472 and $P_{res,2}$ = –649.401659) we obtain Γ_{BW} = 72.2236286, which differs now by almost 7% from the original rate in the cm frame. We are not sure if this discrepancy is related to the similar conclusions of several independent other works [36-39], where the accuracy of the usual Lorentz time dilation formula to describe the internal dynamics of fully interacting systems in a moving frame was questioned. But in our present understanding, the real reason for the observed discrepancy for our rate Γ_{BW} remains an open question. Here we should remind the reader again that we used the Lorentz time dilation pre-factor, that might be strictly valid only for computing the time delay within two identical spatial locations, whereas our Breit-Wheeler rate characterizes the decay of a spatially extended two-photon state.

Alternatively, the loss of the straight forward Lorentz invariance could also be related to the energy-like renormalization that we did in the prior section, when we removed the infinite energy shifts α_1 and (also α_2) from the equations. Similar violations are known from other renormalization schemes. For example, if the momentum cut-off is being used to regularize the uv singularity, the corresponding perturbative expansion is known to violate the Lorentz invariance of decay rates as well. This is in contrast to the dimensional regularization [40], where the invariance of each perturbative term after renormalization is maintained.

We also note that the perturbation theory used in this work is not the same as the Lagrangian-based method used traditionally in high energy physics, where each Feynman diagram manifestly conserves momentum, energy and Lorentz invariance. Our approach, on the other hand, uses the Hamiltonian formalism, which focuses on the generator of the temporal evolution and therefore treats the space-time symmetry in a less transparent way.

As a last point, we should point out the (formal) non-relativistic limit of the Breit-Wheeler rate. This can be obtained if we perform an expansion in inverse powers of the speed of light 1/c. After a lengthy algebra, we obtain the result

$$\Gamma_{BW} = \lambda_4 |P - Q| M_{-1} m_{-2} (m-2M)_{-2} L_{-1} \qquad (5.6)$$

which depends only on the difference of the two final fermion momenta and is therefore Galilean invariant. We note that the mass denominator (m–2M) vanishes at the same time, when the energy and momentum conservation laws for the simple vertex reaction (photon decays into a positron-electron pair) can be satisfied simultaneously, i.e. $K_1 = P'+Q'$ and $\omega_1 = E_{P'} + E_{Q'}$. However, as for most particles the fermionic masses often exceed the bosonic masses, the corresponding four-momentum conservation is typically violated for this

vertex reaction, at least in quantum electrodynamics. The amplification of the rate Γ_{BW} in the limit $(m-2M) \rightarrow 0$ is therefore expected, as the intermediate states (that we adiabatically eliminated) would become resonant. In the center of mass system, where $K_1+K_2 = 0$, such that $|P-Q| = (M/m)^{1/2} |K_1|$, the rate Γ_{BW} increases linearly with incoming photon momentum. Finally, we should remark that one should not physically over-interpret the formal mathematical limit of Γ_{BW} in Eq. (5.6). For example, for $P_{tot} = 0$, the required bare energy resonance condition $\omega_1 = E_{Pres}$ illustrates the intrinsic relativistic nature of the Breit-Wheeler process. The limit $mc^2 = Mc^2$ can only be satisfied for a finite K_1 if m=M, otherwise $K_1 \rightarrow \infty$ is required, which is in contradiction with the limit $c \rightarrow \infty$ used to derive Eq. (5.6).

6. Photon-photon scattering with space-time resolution

6.1 Equations of motion for the amplitudes C(K1,K2,t) and C(P,Q,t)

In the discussion of Sec. 5, the corresponding spatial distribution of the two photons was infinitely extended for $L \rightarrow \infty$. As a result, the reaction rate decreased linearly with the box size L, i.e. $\Gamma_{BW} = v(\lambda,K)\, L^{-1}$. Unlike in a real transient scattering situation, these two particles interacted immediately and constantly with each other, resulting in the exponential decay of the population from a single initial state $|K_1K_2\rangle$ into the set of final states $|PQ\rangle$. In order to simulate more closely the transient nature of the collision of the two photons, we have to choose and initial state where the two particles are spatially localized an initially separated from each other. In contrast to the prior system, where the creation of the electron-positron pairs started instantly, in the transient scattering situation we expect the interaction to occur only during those time intervals, when the two photons overlap, which depend on their initial separation.

The initial spatial localization of each photon can be achieved by a suitable superposition of the states. To be consistent with our normalization of the prior sections, i.e. $\langle\Psi|\Psi\rangle = 1$, we assume here that the photonic momenta are similarly discretized as those of the fermions in a finite box of length L. For example, the single photon state $|\Psi\rangle = \Sigma_K\, G_1(K)\, |K\rangle$, with the unitless amplitude $G_1(K) \equiv (2\pi\, \sigma_{K2})^{-1/4}\, \mathrm{Exp}[-i\, K\, x_1]\, \mathrm{Exp}[-(K-K_0)^2/(4\, \sigma_{K2})]\, \Delta p^{1/2}$ and $\Sigma_K\, |G_1(K)|^2 = 1$ (for $\Delta p \rightarrow 0$) guarantees that the corresponding spatial distribution is Gaussian, centered at $x = x_1$, with an average momentum K_0 and spatial width $\Delta x = 1/(2\sigma_k)$. From now on we assume that Δp is sufficiently small such that for analytical purposes, we can approximate the discrete summation Σ_K by the integral $\Delta p^{-1} \int dK$. We also assume that any spatially localized wave function is negligibly close to the boundary of the finite box.

The spatial properties of $|\Psi\rangle$ can be examined if we compute the photons' spatial density $\rho_\gamma(x)$ from the expectation value of the position-operators, $\rho_\gamma(x) \equiv \langle\Psi|\, a_x^\dagger a_x\, |\Psi\rangle$. Here the spatial annihilation operators are defined by the Fourier transform $a_x \equiv (2\pi)^{-1/2}\, \Delta p^{1/2} \sum_k a_k \exp[i\, k\, x]$. Using $(2\pi)^{-1/2}\, \Delta p \sum_K G_1(K) \exp[i\, K\, x] = 2^{1/4}\, \pi^{-1/4}\, \sigma_{K1/2} \exp[i\, K_0\, (x-x_1)] \exp[\, -(x-x_1)^2\, \sigma_{K2}]$, for the Gaussian amplitude $G_1(K)$, we obtain consistently $\rho_\gamma(x) = (2\pi\Delta x^2)^{-1/2} \exp[\, -(x-x_1)^2 /(2\Delta x^2)]$.

Similarly, in order to examine two spatially localized photons, we use for the initial state

$$|\Psi(t=0)\rangle = \sum_{K1} \sum_{K2} G_1(K_1)\, G_2(K_2)\, |K_1 K_2\rangle \tag{6.1}$$

with the two Gaussian momentum amplitudes

$$G_1(K_1) \equiv (2\pi\ \sigma_{K2})^{-1/4} \exp[-i\, K_1\, x_1] \exp[-(K_1-K_0)^2/(4\, \sigma_{K2})]\, \Delta p^{1/2} \tag{6.2a}$$

$$G_2(K_2) \equiv (2\pi\ \sigma_{K2})^{-1/4} \exp[-i\, K_2\, x_2] \exp[-(K_2+K_0)^2/(4\, \sigma_{K2})]\, \Delta p^{1/2} \tag{6.2b}$$

This particular choice for the momentum amplitudes guarantees that the first (second) photon is located around $x=x_1$ ($x=x_2$) with an average momentum $\langle K_1\rangle = K_0$ ($\langle K_2\rangle = -K_0$) and with initial spatial width $\Delta x = 1/(2\sigma_K)$. In order to avoid any initial spatial overlap, we will choose the separation between both particles to exceed the spatial width of each packet, i.e., $|x_2 - x_1| >> \Delta x_0$.

We note that in contrast to $|\Psi(t=0)\rangle = |K_1 K_2\rangle$, this particular initial state does not have a sharp total momentum anymore. By introducing the Kronecker function $\delta_{K1+K2,Ptot}$ under the twofold sum $\sum_{K1} \sum_{K2}$ … one could achieve a desired sharp total momentum for the two-wave packet combination. However, this would induce (in our opinion rather unnatural) correlations between the two incoming photons, which should actually be independent of each other.

As the total momentum is still conserved, the dynamics can be decomposed into independent subspaces, each for a different P_{tot}. It is therefore sufficient to label the two-particle states by the momentum of one particle and the total momentum, i.e., $|K;P_{tot}\rangle$ ($= |K_1 K_2\rangle$) and $|P;P_{tot}\rangle$ ($= |PQ\rangle$). According to Eq. (6.1), the initial state then is given by $|\Psi(t=0)\rangle = \sum_{Ptot} \sum_K G_1(K)\, G_2(P_{tot}-K)\, |K;P_{tot}\rangle$. Using this notation, the time-evolved scattering state can be expressed as

$$|\Psi(t)\rangle = \Sigma_{Ptot} \{ \Sigma_K C_K(t; P_{tot}) |K;P_{tot}\rangle + \Sigma_P C_P(t; P_{tot}) |P;P_{tot}\rangle \} \quad (6.3)$$

The photonic and fermionic amplitudes $C_K(t; P_{tot})$ and $C_P(t; P_{tot})$ have to fulfill the normalization condition $\Sigma_{Ptot} \Sigma_K |C_K(t; P_{tot})|^2 + \Sigma_{Ptot} \Sigma_P |C_P(t; P_{tot})|^2 = 1$. The time-evolution is predicted by the equations

$$i\, d\, C_K(t;P_{tot})/dt = (\omega_1 + \omega_2)\, C_K(t;P_{tot}) + \Sigma_P\, \Omega(P,K;P_{tot})\, C_P(t;P_{tot}) \quad (6.4a)$$

$$i\, d\, C_P(t;P_{tot})/dt = (E_P + E_Q)\, C_P(t;P_{tot}) + \Sigma_K\, \Omega(P,K;P_{tot})\, C_K(t;P_{tot}) \quad (6.4b)$$

If we compare the structure of these equations with those of a single initial state $C_K(t=0;P_{tot}) = \delta_{K,K1}\, \delta_{Ptot-K1-K2}$ as discussed in Eqs. (5.1), where we introduced for better clarity the total momentum explicitly, we see that the only difference is the additional summation over the amplitudes C_P, i.e., $\Omega(P)\, C_K$ in Eq. (5.1b) versus $\Sigma_K\, \Omega(P,K;P_{tot})\, C_K(P_{tot})$ in Eq. (6.4b). This additional summation has some very serious implications for the time-dependence of C_K. In Eqs. (5.1), the initial probability $|C_K|^2 = 1$ for a single initial state decays immediately, whereas the decay of many states in Eqs. (6.4) from their initial values $G_1(K)\, G_2(P_{tot}\text{-}K)$ is delayed. The amount of this time-delay depends crucially on the other initial amplitudes C_K. This is due to the fact that all (initially non-vanishing) amplitudes C_K for the states $|K;P_{tot}\rangle$ with different values of K are coupled directly to the identical set of electron-positron states $|P;P_{tot}\rangle$. Mathematically, this is reflected by the fact that the source-term for the amplitude C_P in Eq. (6.4b) is given by the *coherent* sum $\Sigma_K\, \Omega(P,K;P_{tot})\, C_K(t;P_{tot})$, which due to the different (K-dependent) complex phases of the amplitudes $C_K(t=0)$ is initially very close to zero. The vanishing source term leads to the fact that at early times, $C_P(t;P_{tot})$ cannot grow and, as a result, C_K cannot decay as its coupling term is identical to zero, as $C_P(t=0;P_{tot})=0$. As we see below, the amount of this resulting delay can be easily interpreted by examining the underlying dynamics from a spatially resolved perspective. We will see that this delay time corresponds precisely to the minimum time both photon wave packets require to overlap spatially.

6.2 Time-dependence of the amplitudes $C_K(t;P_{tot})$ and $C_P(t;P_{tot})$

To be consistent with the restriction to include only processes up to order $O(\lambda_4)$, we can construct the

perturbative solution to Eqs. (6.4). As the source term $\Sigma_P\, \Omega(P,K;P_{tot})\, C_P(t;P_{tot})$ vanishes initially in Eq.(6.4a) we obtain the interaction free time evolution $C_{K(0)}(t; P_{tot}) = \mathrm{Exp}[-i\,(\omega_1 + \omega_2)\, t]\, G_1(K)\, G_2(P_{tot}-K)$. Here we have used the initial amplitudes $C_{K(0)}(t=0; P_{tot}) = G_1(K)\, G_2(P_{tot}-K)$, which are given by Eq. (6.2) and describe the initial spatial locations x_1 and x_2, the initial momentum width σ_k and their initial velocities k_0 and $-k_0$ of the two Gaussian photon wave packets. If we insert the zeroth order solution $C_{K(0)}(t; P_{tot})$ into Eq. (6.4b), the last term on the right hand side does not depend on $C_P(t;P_{tot})$ and has a given time-dependence. It therefore acts as a source term (inhomogeneity). Using the usual Green's function technique [with a vanishing homogeneous solution as $C_P(t=0;P_{tot})= 0$], we obtain the perturbative solution

$$C_{P(1)}(t;P_{tot}) = -i \int_{0t} d\tau\, \mathrm{Exp}[-i\,(E_P + E_{Ptot-P})\,(t-\tau)]\, \Sigma_K\, \Omega(P,K;P_{tot})\, C_{K(0)}(\tau;P_{tot}) \qquad (6.5)$$

Due to the simple exponential time-dependence of $C_{K(0)}(\tau;P_{tot})$, we can perform the time integral leading to

$$\begin{aligned} &\int_{0t} d\tau\, \mathrm{Exp}[-i\,(E_P + E_{Ptot-P})\,(t-\tau)]\, \mathrm{Exp}[-i\,(\omega_1 + \omega_2)\,\tau] \\ &= i\,\big[\mathrm{Exp}[-i\,(E_P + E_{Ptot-P})\,t] - \mathrm{Exp}[-i\,(\omega_1 + \omega_2)\,t]\big] \,/\, \big[(E_P + E_{Ptot-P}) - (\omega_1 + \omega_2)\big] \\ &\equiv F[t,P,K;P_{tot}] \end{aligned} \qquad (6.6)$$

which for the energy resonant case $(E_P + E_Q) = (\omega_1 + \omega_2)$ reduces according to L'Hopital's rule to the simpler form $F[t,P,K;P_{tot}] = t\, \mathrm{Exp}[-i\,(\omega_1 + \omega_2)\, t]$. This means that the solution of Eq. (6.5) can be simplified to a single momentum summation

$$C_{P(1)}(t;P_{tot}) = -i\, \Sigma_K\, F[t,P,K;P_{tot}]\, \Omega(P,K;P_{tot})\, G_1(K)\, G_2(P_{tot}-K) \qquad (6.7)$$

Likewise, if we want to find the time-evolution of the amplitudes of the two-photon state, we can insert $C_{P(1)}(t;P_{tot})$ back into Eq. (6.4a), which also can be solved analytically as

$$\begin{aligned} C_{K(0)}(t;P_{tot}) + C_{K(2)}(t;P_{tot}) = {} & \mathrm{Exp}[-i\,(\omega_1 + \omega_2)\, t]\, G_1(K)\, G_2(P_{tot}-K) - \\ & -i \int_{0t} d\tau\, \mathrm{Exp}[-i\,(\omega_1 + \omega_2)\,(t-\tau)]\, \Sigma_P\, \Omega(P,K;P_{tot})\, C_{P(1)}(\tau;P_{tot}) \end{aligned} \qquad (6.8)$$

Once again, due to the simple exponential time-dependence of $C_{P(1)}(\tau;P_{tot})$, we can perform the time integral leading to

$$F_{12}(t) \equiv \int_{0t} d\tau \, Exp[-i\,(\omega_1 + \omega_2)\,(t-\tau)]\, F[\tau,P,K';P_{tot}]$$

$$= \int_{0t} d\tau \, Exp[-i\,(\omega_1 + \omega_2)\,(t-\tau)]\, i\,\big[Exp[-i\,(E_P + E_Q)\,\tau] - Exp[-i\,(\omega_1' + \omega_2')\,\tau]\,\big] \,/$$

$$\big[(E_P + E_Q) - (\omega_1' + \omega_2')\big]$$

$$= F_1(t) \,/\, \big[(E_P + E_Q) - (\omega_1' + \omega_2')\big] + F_2(t)/\big[(E_P + E_Q) - (\omega_1' + \omega_2')\big] \qquad (6.9)$$

where

$$F_1(t) \equiv -\big[Exp[-i\,(E_P + E_Q)t] - Exp[-i\,(\omega_1 + \omega_2)t]\big]/\big[(E_P + E_Q) - (\omega_1 + \omega_2)\big] \qquad (6.10a)$$

$$F_2(t) \equiv \big[Exp[-i\,(\omega_1' + \omega_2')t] - Exp[-i\,(\omega_1 + \omega_2)t]\big]/\big[(\omega_1' + \omega_2') - (\omega_1 + \omega_2)\big] \qquad (6.10b)$$

This simplifies the final solution to

$$C_{K(0)}(t;P_{tot}) + C_{K(2)}(t;P_{tot}) = Exp[-i\,(\omega_1 + \omega_2)\,t]\; G_1(K)\; G_2(P_{tot}-K)$$

$$- \Sigma_P\; \Omega(P,K;P_{tot})\; \Sigma_{K'}\; F_{12}(t)\; \Omega(P,K';P_{tot})\; G_1(K')\; G_2(P_{tot}-K') \qquad (6.11)$$

Before we discuss the spatial densities of the transient scattering process, we can use the obtained time-dependence of the amplitudes $C_{P(1)}(t;P_{tot})$ to analyze the temporal growth of the total number of the created electron-positron pairs, defined as

$$N_{e\text{-}p}(t) \equiv \Sigma_{Ptot}\, \Sigma_P\, |\langle PP_{tot} \,|\, \Psi(t)\rangle|_2$$

$$= \Sigma_{Ptot}\, \Sigma_P\, \big|C_{P(1)}(t,P_{tot})\big|_2$$

$$= \Sigma_{Ptot}\, \Sigma_P\, \big|\, \Sigma_K\, F[t,P,K;P_{tot}]\; \Omega(P,K;P_{tot})\; G_1(K)\; G_2(P_{tot}-K)\big|_2 \qquad (6.12)$$

In contrast to the linear-time growth of $N_{e\text{-}p}(t) = \Gamma_{BW}\, t$ characteristic for a monochromatic two-photon initial state, i.e. $C_K(t=0;P_{tot}) = \delta_{K,k0}\delta_{Ptot-K,-k0}$, the temporal growth for two initially spatially localized photon wave packets depends rather nontrivially on the initial separation $x_2 - x_1$, on the initial spatial width $1/(2\sigma_K)$ as well as on the relative speed of the two Gaussian photon wave packets.

This transient growth can only occur during the time the two wave packets spatially overlap, reflecting the local nature of the original interaction potential. In Figure 6 we present a numerical example.

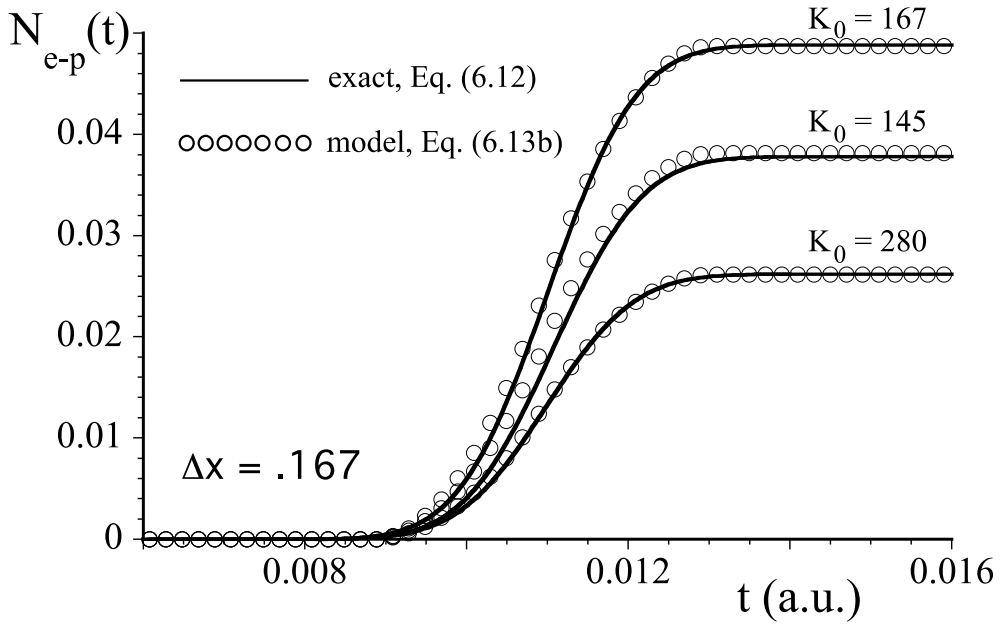

Figure 6 The growth of the electron-positron pair creation probability $\Sigma_{Ptot}\,\Sigma_P\,|\langle PP_{tot}|\Psi(t)\rangle|^2$ as a function of time due to the collision of two photon wave packets. For comparison, the open circles are the predictions according to the simple model of Eq. (6.13) based on the Breit-Wheeler rate obtained in Eq. (5.3). [$\lambda = 1$, fermion mass M = 1 a.u., boson mass m = 0.1 a.u., momentum width $\sigma_k = 3$ a.u. and initial central locations $x_1 = -x_2 = -1.5$ a.u.]

We see that for our relativistic parameters the probability growth is indeed maximal at time $t = (x_2 - x_1)/(2c)$, when the two centers of the wave packets have their maximum overlap. For $K_0 > 145$, the corresponding speed is nearly c. In contrast to the immediate decay for the monochromatic limit, the beginning of the growth of $\Sigma_{Ptot}\,\Sigma_P\,|\langle PP_{tot}|\Psi(t)\rangle|^2$ is delayed depending on the scattering parameters $(x_2 - x_1)$, k_0 and Δx. Depending on the center momentum K_0, the spatial width Δx and the threshold momentum for pair creation [$\omega(K_{min}) = Mc^2$], there are two dynamical scattering regimes of interest.

For the monochromatic limit, where the variation of $\Omega(P,K;P_{tot})$ for $-\sigma_K+K_0 < K < K_0+\sigma_K$ is negligible and $K_{min} < -\sigma_K+K_0$, we can construct an illustrative but approximate analytical model for the time-dependence of $N_{e\text{-}p}(t)$ based on the main expression (5.3) from the spatially independent analysis for a single momentum, i.e., $\Gamma_{BW} = v(\lambda,K)\, L_{-1}$. For simplicity, we assume that the right traveling photon wave packet has a simple rectangular probability distribution $\rho_\gamma(x,t) = 1/(\Delta x)\{\theta(w/2+ x + x_1 - ct)\, \theta(w/2 - x + x_1 + ct) -1]\}$. The left traveling photon corresponds to a $x_2 = -x_1$ and a reversed speed c in the same expression. The L_{-1} dependence of the Γ_{BW} was a result of the delocalization of the two monochromatic waves across the entire numerical box of length L, i.e. $\rho(x) \sim L_{-1}$. This needs to be multiplied with the factor L_2/w_2 to correct for the probability density 1/w for the spatially localized photon, If we divide the resulting total rate $\Gamma_{BW} = v(\lambda,K)\, L/(\Delta x)_2$ by L, we obtain the reaction rate per unit length for the two crossing photons as $v(\lambda,K)\, 1/w_2$. Finally, to obtain $N_{e\text{-}p}(t)$, we multiply this reaction rate with the time-dependent overlap length $L_{over}(t)$ of both packets, given by the triangularly shaped time-dependence centered at $t = c/x_2$, with height w and width w/c. We obtain

$$N_{e\text{-}p}(t) = v(\lambda,K)\, 1/w_2 \int_{-\infty T} d\tau\, L_{over}(\tau) \qquad (6.13a)$$

Using $\int_{-\infty\infty} d\tau\, L_{over}(\tau) = w_2/(2c)$, the asymptotic value after the collision follows as $N_{e\text{-}p}(\infty) = v(\lambda,k)/(2c)$. Interestingly, this final value after the collision is *independent* of the spatial width w, as a result of the perfect cancellation of two competing mechanisms. An increase of the width w has two opposite effects, on the one hand it increases the overlap time, however, it also decreases the probability. More specifically, Eq. (6.13a) can be solved analytically and the time-dependent growth regime of $N_{e\text{-}p}(t)$ is characterized by two regimes. It first increases quadratically in time, which is then followed by the rising portion of an inverted parabola:

$$\begin{aligned}
&N_{e\text{-}p}(t) = 0 && \text{for} \quad t-t_{del} < 0 \\
&N_{e\text{-}p}(t) = v(\lambda,K)\, w_2\, c\, [t-t_{del}]_2 && \text{for} \quad 0 < t-t_{del} < \Delta x_0/(2c) \\
&N_{e\text{-}p}(t) = v(\lambda,K)\, w_2\, c\, \left[1 - 2\, c_2/w_2\, (t—t_{del}-w/c)_2\right] && \text{for} \quad w/(2c) < t-t_{del} < w/c \\
&N_{e\text{-}p}(t) = v(\lambda,K)\, /(2c) && \text{for} \quad w/c < t-t_{del} \qquad (6.13b)
\end{aligned}$$

with the arrival delay time given by $t_{del} \equiv c/x_2$. In order to match the photonic Gaussian distribution with the simple rectangular distribution, we have used as a width $w = 12^{1/2}\,\Delta x_0$, which guarantees that the Gaussian and its rectangular approximation have the same spatial variance. The open circles in Figure 6 represent $N_{e\text{-}p}(t)$ according to the remarkable simple Eq. (6.13b) and the quantitative agreement is quite impressive.

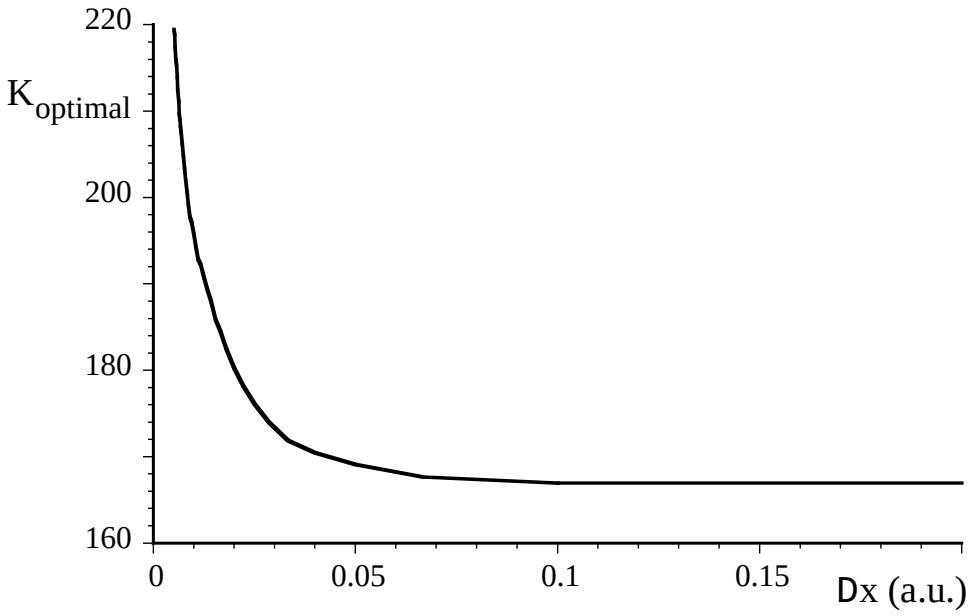

Figure 7 The optimal photon momentum K_{opt} that maximizes the final number of created electron-positron pairs after the scattering process as a function of the spatial width Δx of the photon wave packet. [coupling strength λ=1, fermion mass M=1 a.u., boson mass m=0.1 a.u.]

The opposite (non-monochromatic) scattering limit of strongly localized photons is interesting, as it predicts a "blue shift" of the optimal photon momentum K_{opt} with regard to the spatial width of the photon wave packet Δx. In this regime, the momentum spectrum $G_1(K)$ can contain momenta, that are below the

threshold value K_{min}, i.e., $-1/(2\Delta x) + K_0 < K_{min}$, and are therefore immune to pair creation. The resulting blue shift is illustrated in Figure 7, where we have graphed the optimal photon momentum K_{opt} that maximizes the final number of created electron-positron pairs $N_{e\text{-}p}(t=\infty)$ after the scattering process as a function of Δx. For small widths, i.e., $\Delta x < 0.5(K_0 - K_{min})^{-1}$, we see that the value for the optimum momentum K_{opt} begins to increase with decreasing Δx in order to compensate for the lack of above-threshold momentum contributions.

In Figure 8 we display also a novel coherence effect characteristic of the strong localization of the two wave packets. The simultaneous presence of different momenta associated with a large momentum width [$\sigma_K = 1/(2\Delta x)$] leads to interesting quasi-oscillatory structures that are superimposed on the expected monotonic growth for $N_{e\text{-}p}(t)$ during the collision. For a rough qualtiative comparison with an entirely incoherent description, we have simply added up the solutions from Eq. (6.13b) $N_{e\text{-}p}(t)$ for different momentum pairs with Gaussian weights according to the distribution of the momenta, i.e. $N_{e\text{-}p}(t) = \Sigma_K |G_1(K)|^2 N_{e\text{-}p}(t,K)$. While this prediction agrees very roughly with the overall observed growth pattern of the particle yield, it cannot reproduce the coherent oscillatory pattern.

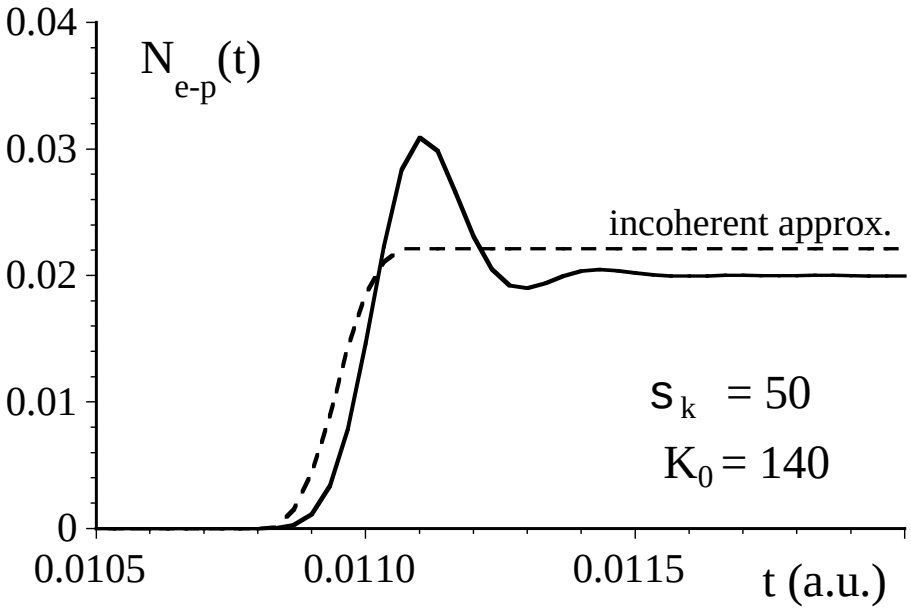

Figure 8 The growth of the electron-positron pair creation probability $\Sigma_{Ptot}\,\Sigma_{P}\,|\langle PP_{tot}|\Psi(t)\rangle|^2$ as a function of time due to the collision of two photon wave packets that are spatially very narrow, corresponding to two localized photons. For comparison, the dashed line is the predictions according to very crude model based on the incoherent superposition of the solutions of Eq. (6.13b) with Gaussian weights. [$\lambda = 1$, $M = 1$ a.u., $m = 0.1$ a.u., $\sigma_k = 50$ a.u., $K_0=140$ a.u., $x_1 = -x_2 = -1.5$ a.u.]

6.3 Spatial densities for the photon and created electron-positron pairs

Finally, in order to examine also the spatial density with regard to the photons, we have to compute $\rho_\gamma(x,t) = \langle\Psi(t)|\, a(x)^\dagger a(x)\,|\,\Psi(t)\rangle$. After straightforward algebra, we obtain

$$\rho_\gamma(x,t) = 1/(2\pi)\,\Sigma_{K2}\,\big|\,\Sigma_{K1}\,C(K_1,K_2,t)\,\mathrm{Exp}(i\,K_1\,x]\,\big|^2 + 1/(2\pi)\,\Sigma_{K1}\,\big|\,\Sigma_{K2}\,C(K_1,K_2,t)\,\mathrm{Exp}(i\,K_2\,x]\,\big|^2 \qquad (6.14)$$

At the initial time, we can use the normalization $\Sigma_K\,|G_i(K)|^2 = 1$ for i=1,2. This reduces the initial density to $\rho_\gamma(x,t=0) = (2\Delta x\,\pi^{1/2})^{-1}\{\mathrm{Exp}\,(-(x-x_1)^2/(2\Delta x_0^2)] + \mathrm{Exp}\,(-(x-x_2)^2/(2\Delta x^2)]\}$ as expected

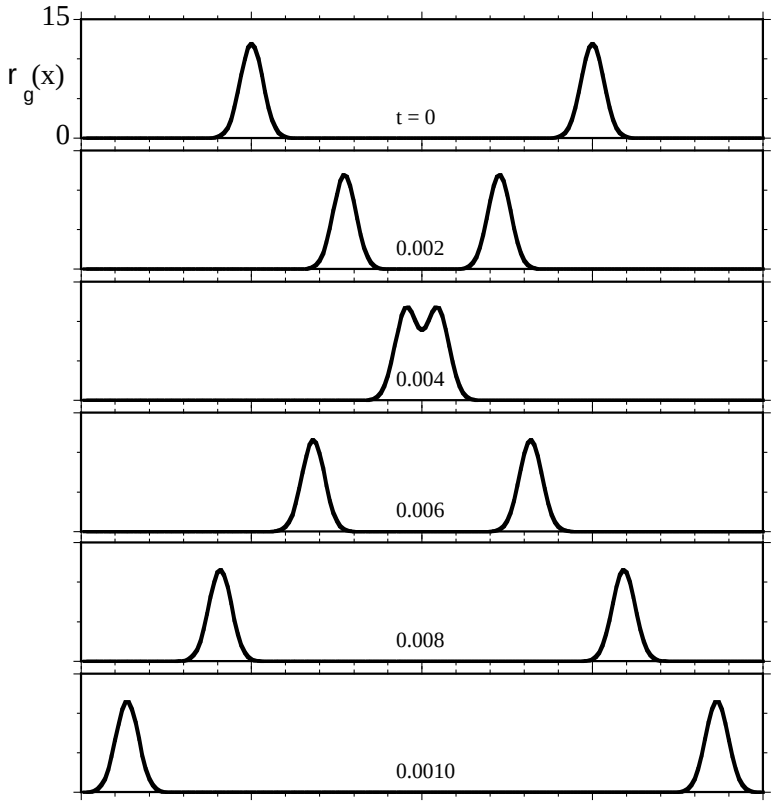

Figure 9 The time-evolution of the spatial distribution $\rho_\gamma(x,t)$ of the two colliding photons [$\lambda = 1$, M=1 a.u., m=0.1 a.u., K_0=150 a.u., σ_k = 15 a.u., $x_1 = -x_2 = -0.5$ a.u.]

In the absence of any coupling, i.e. $C_K(t) = \text{Exp}[-i(\omega_2+\omega_1)\, t]$, the structure of Eq. (6.14) shows that the two wave packets just propagate through each other without any interference when they overlap. We note that the absence or occurrence of interferences in colliding photon wave packets was discussed in a prior work [25]. For the coupled situation ($\Omega \neq 0$) we have to numerically evaluate Eq. (6.14).

In Figure 9 we show the temporal snapshots of the two colliding photon packets. The first two snapshots at t=0 and t=0.002 show the two packets moving towards each other nearly shape invariant. At around t=0.004, the two photon packets start to pass through each other while interacting. During the same time interval electron-positron pairs are created. The frames taken at t=0.006, 0.008, and 0.010 show the two photon packets move away from the interaction zone. The peak of the packets is reduced by a small amount. This height reduction [from $\rho_\gamma(x=\pm 0.5, t=0) = 11.97$ to $\rho_\gamma(x=\pm 0.86, t=0.01) = 11.47$] reflects the photon annihilation associated with the creation of the electron-positron pair. The total area under both densities has

decreased from $\int dx\ \rho\gamma(x,t=0) = 2$ to $\int dx\ \rho\gamma(x,t=0.01) = 1.93$, meaning that 3.5% of the probability of each photon was annihilated. As the packets move basically with the speed of light and the interaction time is short, a further reduction of the peak height due to quantum mechanical spreading is negligible here.

Very similarly, we can also define the spatial probability density of the created electrons and positrons as $\rho_e(x) = \langle\Psi(t)|b(x)\dagger b(x)|\Psi(t)\rangle$ and $\rho_p(x) = \langle\Psi(t)|d(x)\dagger d(x)|\Psi(t)\rangle$, where the corresponding spatial operators b(x) and d(x) are again derived from the corresponding momentum operators by Fourier transformation. Using the solution for (6.4) we obtain

$$\rho_e(x,t) = \rho_p(x,t) = 1/(2\pi)\ \Sigma_Q \left| \Sigma_P\ C_P(t;P_{tot})\ \mathrm{Exp}\ (i\ P\ x) \right|_2 \qquad (6.15)$$

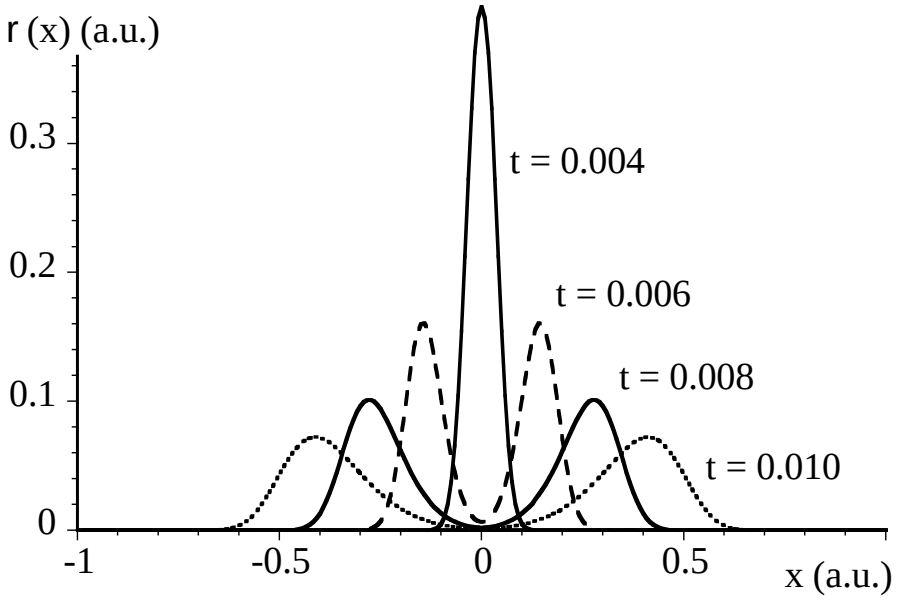

Figure 10 The time-evolution of the spatial distribution $\rho_e(x,t)$ of the created electrons during the two colliding photons. [$\lambda = 1$, M=1 a.u., m=0.1 a.u., $K_0 = 150$ a.u., $\sigma_k = 15$ a.u., $x_1 = -x_2 = -0.5$ a.u.]

We graph the electron's spatial density in Figure 10 for several moments in time ranging from t = 0 to 0.010 a.u. For reasons of symmetry, the corresponding positronic density is identical to that of the electron. Consistent with the data in Fig. 9, the electron density for the early time frames is nearly zero, as photon packets have not yet achieved their spatial overlap. Once the two photons collide, we observe the expected growth close to t =0.004 a.u. After the photon packets have separated and move away from each other, no new electrons (or positrons) are created. But the electron's probability density created at around t = 0.004 splits into two parts and start to move away from the very location where they were created. As the momentum distribution of the outgoing electron wave packets is rather wide, the spatial density spreads. Because we assumed that the electron's mass M was ten times larger than that of the photon, the spatial spreading is significantly larger for the electron than that for the photon. This is obvious from a direct comparison of $\rho_\gamma(x,t)$ (Fig. 9) and $\rho_e(x,t)$ (Fig 10) for the same moments in time. While the peak of the photon packet moves with nearly the speed of light in Fig. 9, the electron propagates out at a lesser speed close to only 67 a.u. This central speed is fully consistent with resonant momentum P_{res} discussed in the prior sections for the given central photon momentum.

7. Summary and open questions

In this work we employed an interacting quantum field theory to analyze the famous Breit-Wheeler process. The present work differs from prior works mainly in two respects. First, it included the back-reaction of the created electron-positron pairs on the colliding photons. Second, the dynamics was examined from a spatially resolved perspective. In order to study the back-reaction we had to go beyond the external field approximation, where the two colliding photons are usually represented in the Dirac equation by an electromagnetic radiation field with a prescribed space-time dependence. In addition to laying out a possible theoretical framework for such an approach, the space-time resolved studies also led to new predictions. For spatially localized photon wave packets we observed an interesting blue shift with regard to the optimum photon momentum that can lead to the largest amount of pair creation. The simultaneous presence of many energy contributions required to have spatially localized photon states also led to novel coherent oscillations in the electron-positron yield during the collision.

However, to make the present approach numerically feasible, we also had to employ several approximations. The most serious of which is likely the restriction to only 1+1 dimensions, which does not permit us to examine angularly resolved scattering properties as well as implications of various spins. We also point out that we presently do not fully understand how the energy shifts associated with the adiabatic

elimination of the off-resonant intermediate states can be compensated with an appropriate charge and mass renormalization. To make analytical predictions, we have employed several simple model approximations, whose range of validity was established with a direct comparison with the quantum field theoretical data.

We should also comment on some energetic aspects of the dynamics. While the momenta of each of the two photons (and therefore the total momentum of the system) were well-defined, the total energy was not. As the Hamiltonian was time-independent, the expectation value of the energy was independent of time. But as the initial two-photon state $|K_1K_2\rangle$ as well as the set of final states $|PQ\rangle$ were not energy eigenstates, the energy uncertainty $\langle\Delta E\rangle$ was non-zero. This means that the usual textbook discussions of cross-sections and decay rates that are usually based on the assumption of a sharp total four-momentum, such as $\omega_1+\omega_2 = E_P+E_Q$, would need to be re-evaluated for our approach.

The space-time approach employed here allows us to probe the interaction zone. Such an intuitive approach should be viewed as being complementary to the more traditional S-matrix approach normally used to calculate the long-time total reaction cross-section. For the S-matrix, the initial two-photon state and the final electron-positron state are required to be fully energy degenerate, but not orthogonal to each other. This is entirely different compared to the spatially resolved approach where neither the initial nor the final state have a well-defined energy and they are mutually orthogonal. It might be interesting to examine the spatial properties of the true (dressed) energy eigenstates in this degenerate sub-space and to relate them to the scattering states examined in this work.

While we focused our attention on a restricted dimensional model, three-dimensional calculations may be required to adequately account for all spatial features of the dynamics of the incoming photons. Nevertheless, we believe the main conclusions from this work will stay valid for the more general Breit-Wheeler process. For example, while this work is theoretical and serves mainly as a first proof of concept, we believe that for example the predicted blue shift and the coherent oscillation features might also be relevant to future experimental investigations. Obviously for detailed comparison with a future experiment, more sophisticated studies with realistic parameters have to be considered.

Acknowledgements

Y.L. would like to thank ILP for the nice hospitality during her visit to Illinois State. We acknowledge helpful discussions with Dr. T.T. Xi, Dr. Y.T. Li and S. Comben. This work has been supported by the NSF, NSFC (Grant No. 11529402) and Research Corporation.

Appendix A

We briefly review here the derivation of the Hamiltonian for our model system and summarize the resulting functional dependence of the eight coupling functions on the momenta of the electrons, positrons and photons. We also give its discretized form that is being used for the numerical calculations. For our numerical applications we use atomic units, for which $\hbar$=1 and c=137.036 a.u.

The usual second-quantization scheme for the fermions is based on the wave function solution $\phi(\mathbf{r},t)$ to the Dirac equation [41], $i\, d\phi(\mathbf{r},t)/dt = (c\, \alpha\, \mathbf{p} + mc^2\, \beta)\, \phi(\mathbf{r},t)$, which can be expressed as a superposition of eigenstates with positive and negative eigenvalues. If we restrict the spatial dimension to 1 (the z-axis) and permit only states that have a sharp spin $\langle S_z \rangle = 1/2$, then the expansion of the fermionic field operator is given at time t=0 by

$$\Psi(z) = \int dp\, (2\pi)^{-1/2}\, b(p)\, \exp(i\, p\, z)\, U_p + \int dq\, (2\pi)^{-1/2}\, d(-q)^{\dagger}\, \exp(i\, q\, z)\, D_q \qquad \text{(A.1a)}$$

where the four-component spinors are given by $U_p \equiv N_p\{1,0,pc/(Mc^2+E_p),0\}$ and $D_q \equiv N_q\{1,0,qc/(Mc^2-E_q),0\}$, where the two normalization factors $N_{u,p} \equiv [1+p^2c^2/(Mc^2+E_p)^2]^{-1/2}$ and $N_{d,q} \equiv [1+q^2c^2/(Mc^2-E_q)^2]^{-1/2}$ guarantee the normalization $U_p^{\dagger}\cdot U_p = D_q^{\dagger}\cdot D_q = 1$. We note that we have formally renamed the annihilation operator b(p) for negative energy states as $d(-q)^{\dagger}$.

As we discuss the spatial probability distributions in this article, we should mention that the field operator $\Psi(z)$ can be used to recover the corresponding single-electron wave function ϕ from the field-theoretical state $b(p)^{\dagger}\,|vac\rangle$ via $\langle vac\,|\,\Psi(z)\, b(p)^{\dagger}\,|vac\rangle = (2\pi)^{-1/2}\exp(i\, p\, z)\, U_p$. Similarly, the wave function associated with the state $d(q)^{\dagger}\,|vac\rangle$, requires the charge conjugated field operator Ψ_c, defined by the anti-unitary operation $\Psi_c \equiv C\,[\Psi^{\dagger}]^T$. Here T denotes the transposed spinors, and C is an anti-symmetric 4×4 matrix that fulfills $C = -C^{-1} = -C^{\dagger} = -C^T$. Based on the usual 4×4 gamma matrices it can be represented by $C \equiv i\,\gamma^2\,\gamma^0$. It can transform the gamma matrices as $C\,\gamma^i\,C^{-1} = -\gamma^{iT}$. The charge conjugated field takes the form [42]

$$\Psi_c(z) = \int dp\, (2\pi)^{-1/2}\, b(p)^{\dagger}\, \exp(-i\, p\, z)\, C\, U_p + \int dq\, (2\pi)^{-1/2}\, d(-q)\, \exp(-i\, q\, z)\, C\, D_q \qquad \text{(A.1b)}$$

If we include the time-dependence, then $\Psi_c(z)$ satisfies the Dirac equation for a positron. The positronic wave

function associated with $d(q)^\dagger |vac\rangle$ can be obtained as $\langle vac |\Psi_c\, d(q)^\dagger |vac\rangle = (2\pi)^{-1/2} \exp(i\, q\, z)\, C\, D_{-q}$, which is consistent with a positive-energy eigenstate with spin $\langle S_z\rangle = -1/2$, as we have $C\, D_{-q} = N_{u,q}\{0,1,0,qc/(Mc^2+E_q)\}$. This shows that the choice for the original electron-positron field operator $\Psi(z)$ in Eq. (A.1a) describes electrons and positrons with opposite spins along the propagation direction. Due to the restriction of the spin parallel to the propagation direction and the confinement to only one spatial dimension, which we call the x-axis from now on, we can omit the two vanishing spinor components and introduce an effective Dirac Hamiltonian by a simple 2×2 operator $c\, p\, \sigma_1 + M\, c^2\, \sigma_3$, that is based on the Pauli matrices and acts on the two-component spinors of the fermionic operator. The corresponding reduced form of the matrix α_3, required for the calculation of the current density operator, reduces here to σ_3.

Let us now examine the interaction with the model photon field. In general, the interaction energy operator takes the form $V_{tot} \sim \int d^3r\, (\gamma_0\Psi)^\dagger\, \gamma_\mu A_\mu\, \Psi$, where γ_μ denote the usual 4×4 matrices. However, as a consequence of our particular fermionic spin choices, in the temporal gauge ($A_0=0$), only the z-component of the vector potential contributes to the energy. This corresponds to a vanishing photon spin along the propagation direction. We rename the one-dimensional position as x and (arbitrarily) chose the interaction energy operator in this model to be of the form $V_{tot} = \lambda\, c^{3/2} \int dx\, \Psi^\dagger\, \sigma_3\, A\, \Psi$, where the bosonic field operator is given in terms of the momentum mode decomposition by

$$A(x) = \int dk\, c\, (4\pi\omega_k)^{-1/2}\, [a(k)\, \exp(i\, k\, x) + a(k)^\dagger\, \exp(-i\, k\, x)] \qquad (A.2)$$

If we insert the two fields Ψ and A into the expression for interaction energy V_{tot} and multiply the products of the sums, we obtain eight terms as $\Psi^\dagger$, Ψ as well as A are given by two sums each. Momentum conservation follows for each vertex reaction from the spatial integration. The momentum dependence of the coupling strength is associated with the scalar products of the corresponding spinors, which we define as $\Gamma_{UU}(p,p',k) \equiv U_p^\dagger \cdot\sigma_3\, U_{p'}\, (4\pi\omega_k)^{-1/2}$, $\Gamma_{UD}(p,q,k) \equiv U_p^\dagger \cdot\sigma_3\, D_q\, (4\pi\omega_k)^{-1/2}$, and $\Gamma_{DD}(q,q',k) \equiv D_q^\dagger \cdot\sigma_3\, D_{q'}\, (4\pi\omega_k)^{-1/2}$. Despite the variety of the eight different coupling mechanisms, in addition to the momentum exchange symmetries $\Gamma_{UD}(q,p,k) = \text{sign}(pq)\, \Gamma_{UD}(p,q,k)$, and the symmetries $\Gamma_{DD}(q,q',k) = -\text{sign}(qq')\, \Gamma_{UU}(q,q',k)$ and $\Gamma_{DU}(q,p,k) = \Gamma_{UD}(p,q,k)$, all eight couplings can be expressed in terms of Γ_{UU} or Γ_{DU} that take the simplified form

$$\Gamma_{UU}(p,p',k) \equiv\ [E(p)E(p') + M^2c^4 - pp'c^2]^{1/2}\, [8\pi\omega(k)\, E(p)\, E(p')]^{-1/2} \qquad (A.3a)$$

$$\Gamma_{UD}(p,q,k) \equiv \text{sign}(p/q+1)\,[E(p)E(q) - M^2c^4 + pqc^2]^{1/2}\,[8\pi\omega(k)\,E(p)\,E(q)]^{-1/2} \qquad \text{(A.3b)}$$

where $\text{sign}(x) \equiv x/|x|$.

To take a concrete example, one of the eight interaction terms is given by

$$V_3 = \lambda\, c^{5/2} \int dx\, (2\pi)^{-1/2} \{\int dp'\, (2\pi)^{-1/2}\, b(p')\, U_p \exp(i\, p'\, x)^\dagger \cdot \sigma_3 \int dk\, c\, (2\pi\omega_k)^{-1/2}\, a(k) \exp(i\, k\, x)$$
$$(2\pi)^{-1/2} \int dq\, (2\pi)^{-1/2}\, d(-q)^\dagger\, D_q \exp(i\, q\, x)\} \qquad \text{(A.4)}$$

It is the result of multiplying the electronic part of $\Psi^\dagger$ with the photonic annihilation part of A and the positronic part of Ψ. Using the orthogonality of the plane waves, the spatial integration leads to non-vanishing terms only if $-p' + k - q = 0$. We therefore only need to compute $U_p{}^\dagger \cdot \sigma_3\, D_{-(k-p)}\, (2\pi\omega_k)^{-1/2}$, which is defined as the coupling function $\Gamma_{UD}(p,p-k,k)$. If we perform the same procedure for all eight terms, we obtain

$$V_1 = \lambda\, c^{5/2} \int dp \int dk\, \Gamma_{UU}(p,p-k,k)\; b(p)^\dagger\, b(p-k)\, a(k) \qquad \text{(A.5a)}$$
$$V_2 = \lambda\, c^{5/2} \int dp \int dk\, \Gamma_{UU}(p,p+k,k)\; b(p)^\dagger\, b(p+k)\, a(k)^\dagger \qquad \text{(A.5b)}$$
$$V_3 = \lambda\, c^{5/2} \int dp \int dk\, \Gamma_{UD}(p,p-k,k)\; b(p)^\dagger\, d(-p+k)^\dagger\, a(k) \qquad \text{(A.5c)}$$
$$V_4 = \lambda\, c^{5/2} \int dp \int dk\, \Gamma_{UD}(p,p+k,k)\; b(p)^\dagger\, d(-p-k)^\dagger\, a(k)^\dagger \qquad \text{(A.5d)}$$
$$V_5 = \lambda\, c^{5/2} \int dp \int dk\, \Gamma_{DU}(p+k,p,k)\; d(-p-k)\, b(p)\, a(k) \qquad \text{(A.5e)}$$
$$V_6 = \lambda\, c^{5/2} \int dp \int dk\, \Gamma_{DU}(p-k,p,k)\; d(-p+k)\, b(p)\, a(k)^\dagger \qquad \text{(A.5f)}$$
$$V_7 = \lambda\, c^{5/2} \int dp \int dk\, \Gamma_{DD}(-p,-p-k,k)\; d(p)\, d(p+k)^\dagger\, a(k) \qquad \text{(A.5g)}$$
$$V_8 = \lambda\, c^{5/2} \int dp \int dk\, \Gamma_{DD}(-p,-p+k,k)\; d(p)\, d(p-k)^\dagger\, a(k)^\dagger \qquad \text{(A.5h)}$$

where the coupling functions Γ are not independent of each other.

With regard to its computational implementation, we can discretize the momentum space with a mode spacing given by $\Delta p = 2\pi/L$, which is equivalent to having a physical system of finite spatial extension L. This parameter permits us to compute finite size effects (such as in cavity QED) in quantum field theory [22] as well as predict the quantities for the special case of an infinitely extended system, $L \to \infty$.

This step introduces also the unitless (discretized) operators on the momentum grid as $b_p \equiv b(p)\, \Delta p^{1/2}$. For simplicity, we use the same grid also for the photonic operators, i.e., $\Delta p = \Delta k$. This leads automatically to

the unitless (anti-)commutator relationships, for example, $[b_p,b_{p'}{}^\dagger]_+ = \delta_{pp'}$. While the diagonal energy integrals in the Hamiltonian turn into simple sums over the momentum, i.e., $\int dp\, E_p\, b(p)^\dagger\, b(p) = \Sigma_p\, E_p\, b_p{}^\dagger\, b_p$, the off-diagonal interaction terms, which contain products of three operators, pick up a scaling factor, for example, the first interaction energy of Eq. (A.5a) becomes $V_1 = \lambda\, \Delta p^{1/2}\, c^{5/2}\, \Sigma_p\, \Sigma_k\, \Gamma^{UU}(p,p-k,k)\, b_p{}^\dagger\, b_{p-k}\, a_k$, such that $\lambda\, \Delta p^{1/2}\, c^{5/2}$ could be interpreted as an effective L-dependent coupling constant for the discretized system. However, as we will see in this work, the occurrence of $\Delta p^{1/2}$ in the coupling energy does not lead to any unphysical results. In fact, we will see that for a fixed value of λ, all scattering data will not depend on Δp in the continuum limit $\Delta p \to 0$, corresponding to $L \to \infty$. This universality was already demonstrated for the L-independent dressing of energies [43] as well as the scaling of bound-state energies in the strong coupling regime. [22]

We should also mention that in order to be consistent, the any basis state also need to be normalized based on the Kronecker delta function, for example $\langle p\, q\, |p'\, q'\rangle = \delta_{pp'}\, \delta_{qq'}$. Using these basis states, the state can be expanded as

$$|\Psi(t)\rangle = C_{\omega_1\omega_2}(t)\, |K_1K_2\rangle + \Sigma_p\, C_{e^-e^+}(p,t)\, |p\, q\rangle + \Sigma_p\, C_{K1}(p,t)\, |p\, q\, K_1\rangle + \Sigma_p\, C_{K2}(p,t)\, |p\, q\, K_2\rangle \qquad (A.6)$$

where the corresponding value for the positron momentum q follows from momentum conservation. This means $q \equiv K_1+K_2-p$ for $|p\, q\rangle$, $q \equiv K_2-p$ for $|p\, q\, K_1\rangle$ and $q \equiv K_1-p$ for $|p\, q\, K_2\rangle$. This state has to satisfy the equation $i\, d|\Psi(t)\rangle/dt = H\, |\Psi(t)\rangle$. If expansion (A.6) is inserted into this equation, and scalar multiplied with the corresponding basis state, we obtain the following set of equations of motion for the expansion amplitudes:

$$\begin{aligned} i\, dC_{\omega_1\,\omega_2}/dt &= (\omega_1 + \omega_2)\, C_{\omega_1\omega_2} + \Sigma_p\, \langle K_1K_2|V_6|p\, q{=}K_2{-}p\, K_1\rangle\, C_{K1}(p) \\ &\quad + \Sigma_p\, \langle K_1K_2|V_6|p\, q{=}K_1{-}p\, K_2\rangle\, C_{K2}(p) \qquad (A.7a) \\ i\, dC_{K1}(p)/dt &= (E_p + E_{q=K2-p} + \omega_1)\, C_{K1}(p) + \langle p\, q{=}K_2{-}p\, K_1|V_3|K_1\, K_2\rangle\, C_{\omega_1\omega_2} \\ &\quad + \langle p\, q{=}K_2{-}p\, K_1|V_2|p{+}K_1\, q{=}K_2{-}p\rangle\, C_{e^-e^+}(p{+}K_1) \\ &\quad + \langle p\, q{=}K_2{-}p\, K_1|V_8|p\, q{=}K_1{+}K_2{-}p\rangle\, C_{e^-e^+}(p) \qquad (A.7b) \\ i\, dC_{K2}(p)/dt &= (E_p + E_{q=K1-p} + \omega_2)\, C_{K2}(p) + \langle p\, q{=}K_1{-}p\, K_2|V_3|K_1\, K_2\rangle\, C_{\omega_1\omega_2} \\ &\quad + \langle p\, q{=}K_1{-}p\, K_2|V_2|p{+}K_2\, q{=}K_1{-}p\rangle\, C_{e^-e^+}(p{+}K_2) \end{aligned}$$

$$+ \langle p\ q=K_1-p\ K_2|V_8|p\ q=K_1+K_2-p \rangle\ C_{e-e+}(p) \qquad \text{(A.7c)}$$

$$i\, dC_{e-e+}(p)/dt = (E_p + E_{q=K1+K2-p})\ C_{e-e+}(p)$$
$$+ \langle p\ q=K_1+K_2-p|V_7|p\ q=K_2-p\ K_1\rangle\ C_{K1}(p)$$
$$+ \langle p\ q=K_1+K_2-p|V_1|p-K_1\ q=K_1+K_2-p\ K_1\rangle\ C_{K1}(p-K_1)$$
$$+ \langle p\ q=K_1+K_2-p|V_7|p\ q=K_1-p\ K_2\rangle\ C_{K2}(p)$$
$$+ \langle p\ q=K_1+K_2-p|V_1|p-K_2\ q=K_1+K_2-p\ K_2\rangle\ C_{K2}(p-K_2) \qquad \text{(A.7d)}$$

where the transition matrix elements based on V_6, V_3, V_2, and V_8 are related to each other via

$$\langle K_1K_2|V_6|p\ q=K_2-p\ K_1\rangle = g\ \Gamma_{DU}(p-K_2,p,K_2) \equiv \gamma(p, K_2) \qquad \text{(A.8a)}$$

$$\langle K_1K_2|V_6|p\ q=K_1-p\ K_2\rangle = g\ \Gamma_{DU}(p-K_1,p,K_1) = \gamma(p, K_1) \qquad \text{(A.8b)}$$

$$\langle p\ q=K_2-p\ K_1|V_3|K_1\ K_2\rangle = g\ \Gamma_{UD}(p,p-K_2,K_2) = \gamma(p, K_2) \qquad \text{(A.8c)}$$

$$\langle p\ q=K_2-p\ K_1|V_2|p+K_1\ q=K_2-p\rangle = g\ \Gamma_{UU}(p,p+K_1,K_1) \equiv \kappa(p, K_1) \qquad \text{(A.8d)}$$

Furthermore if we use $\Gamma_{DD}(q,q',k) = -\,\text{sign}(qq')\,\Gamma_{UU}(q,q',k)$, we obtain

$$\langle p\ q=K_2-p\ K_1|V_8|p\ q=K_1+K_2-p\rangle = -\,g\ \Gamma_{DD}(p-K_1-K_2,p-K_2,K_1)$$
$$= \text{sign}[(p-K_1-K_2)(p-K_2)]\ \ \Gamma_{UU}(p-K_1-K_2,p-K_2,K_1)$$
$$= \text{sign}[(p-K_1-K_2)(p-K_2)]\ \ \kappa(p-K_1-K_2, K_1) \qquad \text{(A.8e)}$$

and similarly

$$\langle p\ q=K_1-p\ K_2|V_3|K_1\ K_2\rangle = g\ \Gamma_{UD}(p,p-K_1,K_1) \equiv \gamma(p, K_1) \qquad \text{(A.8f)}$$

$$\langle p\ q=K_1-p\ K_2|V_2|p+K_2\ q=K_1-p\rangle = g\ \Gamma_{UU}(p,p+K_2,K_2) = \kappa(p, K_2) \qquad \text{(A.8g)}$$

$$\langle p\ q=K_1-p\ K_2|V_8|p\ q=K_1+K_2-p\ \rangle = -\,g\ \Gamma_{DD}(p-K_1-K_2,p-K_1,K_2)$$
$$= \text{sign}[(p-K_1-K_2)(p-K_1)]\ \ \kappa(p-K_1-K_2, K_2) \qquad \text{(A.8h)}$$

$$\langle p\ q=K_1+K_2-p|V_7|p\ q=K_2-p\ K_1\rangle = -\,g\ \Gamma_{DD}(p-K_2,p-K_1-K_2,K_1)$$
$$= \text{sign}[(p-K_1-K_2)(p-K_2)]\ \ \kappa(p-K_1-K_2, K_1) \qquad \text{(A.8i)}$$

Based on the symmetry $\Gamma_{UU}(p,p',K) = \Gamma_{UU}(p,p',-K)$ we simplify furthermore

$$\langle p\ q=K_1+K_2-p|V_1|p-K_1\ q=K_1+K_2-p\ K_1\rangle = g\ \Gamma_{UU}(p,p-K_1,K_1) = \kappa(p, -K_1) \qquad \text{(A.8j)}$$

$$\langle p\ q=K_1+K_2-p|V_7|p\ q=K_1-p\ K_2\rangle = -g\,\Gamma_{DD}(p-K_1,p-K_1-K_2,K_2)$$
$$= \text{sign}[(p-K_1-K_2)(p-K_1)]\ \ \kappa(p-K_1-K_2, K_2)$$

$$\langle p\ q=K_1+K_2-p|V_1|p-K_2\ q=K_1+K_2-p\ K_2\rangle = g\,\Gamma_{UU}(p,p-K_2,K_2) = \kappa(p,-K_2) \qquad \text{(A.8k)}$$

The introduction of the couplings κ and γ simplifies the compact notation used in Eqs. (3.2).

Before closing this appendix, we note a fundamental and non-trivial issue. The model is based on two major restrictions, the first one is to consider only electrons and positrons that are created along the z-direction making all predictions only qualitative with regard to real collisions. The second and most consequential approximation is that the Hilbert space of the fermions is restricted to electrons with spin $S_z = +1/2$ and to positrons with spin $S_z = -1/2$. We have omitted the states $e_-[S_z = -1/2]$ and $e_+[S_z = +1/2]$. As a consequence, [in the temporal gauge $A(0) = 0$] only the fourth component $A_z(z)$ of the four vector plays an active role in the dynamics, as the interaction energy integral does not depend on the two transverse components A_x and A_y.

The impact (and also possible steps towards improvements) to the restriction of the fermionic subspace of states can be most directly analyzed if we consider the required conservation of the total spin S_z along the propagation direction. Due to the omission of the states $e_-[-1/2]$ and $e_+[+1/2]$, the only possible two-photon annihilation process is $\gamma[0] + \gamma[0] \rightarrow e_-[+1/2] + e_+[-1/2]$, based on scalar photons γ with spin $S_z = 0$. In contrast, the more physical process (based on vector photons with helicity $S_z = \pm 1$) $\gamma\,[+1] + \gamma[-1] \rightarrow e_-[+1/2] + e_+[-1/2]$, requires as an intermediate step the vertex reaction $\gamma\,[+1] \rightarrow e_-[+1/2] + e_+[+1/2]$ or $\gamma\,[-1] \rightarrow e_-[-1/2] + e_+[-1/2]$. Our model would therefore only permit us to examine the more physical process as well if we had included electrons with spin $S_z = -1/2$ and positrons with spin $S_z = +1/2$ to the Hilbert space of states.

The key question is therefore how the predictions of our model for the two processes $\gamma[0] + \gamma\,[0] \rightarrow e_-[+1/2] + e_+[-1/2]$ and (II) $\gamma\,[+1] + \gamma\,[-1] \rightarrow e_-[+1/2] + e_+[-1/2]$ would differ. The formal procedural steps discussed in this work involving the adiabatic elimination of the intermediate e_--e_+-γ states, the possibility of a Fermi-Golden Rule analysis and the perturbative treatment can be performed also in a similar fashion for process (II). For example, the key equations (3.2), (4.5), (5.1), (6.4) would be qualitatively the same. The only quantitative difference between (I) and (II) would be that the corresponding coupling matrix elements Γ would take possibly different numerical values.

Appendix B

In this Appendix, we summarize the derivation of the analytical, but approximate solution to the coupled set of equations (4.5) for the amplitude $C_K(t)$ of the state $|K_1K_2\rangle$ as well as the amplitudes $C_P(t)$ associated with the set of states $|PQ\rangle$. This set

$$i\, dC_K/dt = (\omega_1+\omega_2)\, C_K + \Sigma_P\, \Omega(P)\, C_P \qquad \text{(B.1a)}$$

$$i\, dC_P/dt = \Omega(P)\, C_K + [E_P+E_Q]\, C_P \qquad \text{(B.1b)}$$

[under the neglect of the general energy shifts α_1 and $\alpha_2(P)$] can be solved analytically using the dominant-pole approximation. We first transform the amplitudes to Laplace space [44] incorporating the initial values $C_K(t=0) = 1$ and $C_P(t=0) = 0$, leading to

$$i\, s\, C_K(s) - i = (\omega_1+\omega_2)\, C_K(s) + \Sigma_P\, \Omega(P)\, C_P(s) \qquad \text{(B.2a)}$$

$$i\, s\, C_P(s) = \Omega(P)\, C_K + [E_P+E_Q]\, C_P(s) \qquad \text{(B.2b)}$$

The second algebraic equation can be solved leading to $C_P(s) = \Omega(P)\, /[i\, s - (E_P+E_Q)]\, C_K$, which we can insert into the RHS of Eq. (B.2a). If we solve this equation for $C_K(s)$ we obtain

$$C_K(s) = i\, \left[i\, s - (\omega_1+\omega_2) - \Sigma_P\, \Omega(P)_2\, /[i\, s - (E_P+E_Q)] \right]_{-1} \qquad \text{(B.3)}$$

In order to simplify the required inverse Laplace transform, we can apply the dominant pole approximation, where the Laplace variable s in the denominator of the momentum integral is replaced by the "dominant" pole $s = -\, i\, (\omega_1+\omega_2)$.

Next we invoke the continuum approximation to evaluate this summation $\Sigma_P \rightarrow (\Delta p)_{-1} \int dP$. We introduce the energy density of states, defined as the number of states per energy, $\rho(E_P+E_Q) = (d(E_P+E_Q)/dp)_{-1} = c_{-2}\, \{p/E_P - Q/E_Q\}_{-1}$. We therefore obtain $\int d\Omega(P)_2\, /[(\omega_1+\omega_2) - (E_P+E_Q)] = \int de\, \rho(e)\, \Omega(P(e))_2/[(\omega_1+\omega_2 - e]$. Furthermore, as the denominator in our integrand f(x) in our case is analytic in the upper complex half-plane and vanishes fast enough that the integral can be constructed by an infinite semicircular contour, we can apply $\lim \varepsilon\rightarrow 0 \int dx\, f(x)/(x - x_0 + i\varepsilon) = -\, i\, \pi\, f(x_0) + P\int dx\, f(x)/(x-x_0)$, where $P\int$ denotes the principal value of the integral defined as $P\int \equiv \lim R\rightarrow\infty \int_{-R}^{R}$. As a result, the simplified integral can be separated into the residue and the principal part

$$\int de\, \rho(e)\, \Omega(P)_2/[\omega_1+\omega_2 - e] = i\, \pi\, \rho(E_{Pres,1})\, \Omega(P_{res,1})_2 + i\, \pi\, \rho(E_{Pres,2})\, \Omega(P_{res,2})_2 + \chi \qquad \text{(B.4)}$$

where χ denotes the principal part of the integral. The most important parameter of this derivation, $\Gamma_{BW} \equiv 2\pi [\rho(E_{Pres,1})\, \Omega(P_{res,1})^2 + \rho(E_{Pres,2})\, \Omega(P_{res,2})^2]\, (\Delta p)^{-1}$ is the Breit-Wheeler decay rate of the two-photon state. The two resonant momenta are obtained as the solutions of the equation $[(\omega_1+\omega_2) - (E_P+E_Q)] = 0$. If we apply the inverse Laplace transform to Eq. (B3) we obtain the final solution

$$C_K(t) = \mathrm{Exp}[-i\,(\omega_1+\omega_2)t]\, \mathrm{Exp}[-\Gamma_{BW}\, t/2] \qquad (B.5)$$

To obtain the time-evolution for the other set of amplitudes $C_P(t)$, Eq. (B.1b) can be solved using the Green's function, i.e., $C_P(P) = -i\,\Omega(P) \int_t d\tau\, \mathrm{Exp}[-i(E_P+E_Q)(t-\tau)]\, C_K(\tau)$. If we insert the solution for $C_K(\tau)$ from Eq. (B.4) we obtain

$$C_P(t) = -i\,\Omega(P)\, \mathrm{Exp}[-i(E_P+E_Q)t] \int_t d\tau\, \mathrm{Exp}[i\,\Delta E\, \tau]\, \mathrm{Exp}[-\Gamma_{BW}\, \tau/2] \qquad (B.6)$$

where we have defined the energy difference $\Delta E = (E_P+E_Q)-(\omega_1+\omega_2)$. If we perform the integration over time from $\tau=0$ to t, we obtain

$$C_P(t) = -\Omega(P)\, \mathrm{Exp}[-i(E_P+E_Q)t]\, \left[\mathrm{Exp}[i\,(\Delta E + i\,\Gamma_{BW}/2)\, t] - 1\right] / (\Delta E + i\,\Gamma_{BW}/2) \qquad (B.7)$$

Appendix C Using Fermi's Golden rule to approximate the Breit-Wheeler rate Γ_{BW}

The "coupling to a single final state approximation" can also be used to construct the Breit-Wheeler rate alternatively via the traditional Fermi-Golden rule approach [35]. The solutions (4.7) describe the transfer of the initial state $|K_1K_2\rangle$ to a set of states $|PQ\rangle$ for all times. If the set of states $|PQ\rangle$ is discrete, we saw in Section 4.2 that this would predict an oscillatory feedback between this set and $|K_1K_2\rangle$, characterized by discrete eigen-energies. However, if the amplitude for $|K_1K_2\rangle$ is coupled to a continuum of states, it can decay irreversibly due to the destructive interference between the oscillating frequencies for each member of the continuum. In this case the usual Golden Rule might become applicable permitting us to determine a characteristic exponential decay rate for $|K_1K_2\rangle$, which is identical to the electron-positron pair creation rate for this Breit-Wheeler process. To determine this rate, we can follow the usual approach that has been used several decades ago to analyze the ionization problem [45]. In order to obtain a transition probability, we have to sum this particular probability density $|C_P(t)|^2$ over all possible final states with different momenta P. Using the continuum approximation to evaluate this summation, we introduce the energy density of states, defined as the number of states per energy, $\rho(E) = dP/dE$. As we saw above in Section 4.2.2, if we consider only a single final state Prob ($|K_1K_2\rangle \rightarrow |PQ\rangle$), then we have in the perturbative limit ($\Omega << \Delta E$)

$$|C_P(t)|^2 = 4\,\Omega^2\,\mathrm{Sin}^2(\gamma t/2)/\gamma^2 \approx 4\,\Omega^2\,\mathrm{Sin}^2(\Delta E\, t/2)/\Delta E^2 \qquad (C.1)$$

If we sum this result over all final states, we could define a probability to excite any final state as $\mathrm{Prob}_{all} = \Sigma_P |C_P(t)|^2$. If we use the continuum approximation [$\Sigma_P \rightarrow (\Delta p)^{-1}\int dP$] to evaluate this discrete summation and change the integration variable to the energy, we obtain $\mathrm{Prob}_{all} \approx (\Delta p)^{-1} \int dE\ \rho(E)\ 4\,\Omega^2\,\mathrm{Sin}^2(\Delta E\, t/2)/\Delta E^2$. As the simultaneous presence of an infinite set of final states leads to a different time evolution of $|C_1(t)|^2$ than obtained in Eq. (4.7c), this expression for Prob_{all} is only a short-time approximation. If we assume that the time t is nevertheless sufficiently long and the energy density $\rho(E)$ ($\equiv dp/dE$) and $\Omega(P)$ varies slowly with E around the two resonant energies, we can factor out these two terms from the integral. They are evaluated for the momenta where ΔE vanishes, $\rho(E) \rightarrow \rho_{res,i}$ and $\Omega(E) \rightarrow \Omega_{res,I}$ with i=1,2. The remaining integral is of the form $\int dx\ \mathrm{Sin}(x\, t/2)^2/x^2 = \pi\, t/2$. As a result, we obtain $\mathrm{Prob}_{all} = 2\pi\ [\rho_{res,1}\,\Omega_{res,1}^2 + \rho_{res,2}\,\Omega_{res,2}^2]\ (\Delta p)^{-1}\, t$, such that we would interpret the prefactor as the pair-creation rate Γ_{BW}. We discuss the dependence of this Breit-Wheeler decay rate Γ_{BW} on the initial photon momentum and the fermionic and bosonic masses for our

model in more detail in Section 5. If we neglect the λ-dependence of the resonant momentum P_{res}, then Γ_{BW} scales quartically in λ, as expected.

References

[1] G. Breit and J.A. Wheeler, Phys. Rev. 46, 1087 (1934).

[2] Nikishov, A.I. Zhur. Eksptl'. I Teoret. Fiz. 41 (1961).

[3] H.R. Reiss, J. Math. Phys. 3, 59 (1962).

[4] A.I. Nikishov and V. I. Ritus, Sov. Phys. JETP 19, 529 (1964).

[5] N.B. Narozhny, A.I. Nikishov and V.I. Ritus, Sov. Phys. JETP 20, 622 (1965).

[6] D.L. Burke, R.C. Field, G. Horton-Smith, J.E. Spencer, D. Walz, S.C. Berridge, W.M. Bugg, K. Shmakov, A.W. Weidemann, C. Bula, K.T. McDonald, E.J. Prebys, C. Bamber, S.J. Boege, T. Koffas, T. Kotseroglou, A.C. Melissinos, D.D. Meyerhofer, D.A. Reis and W. Ragg, Phys. Rev. Lett. 79, 1626 (1997);

[7] C. Bula, K.T. McDonald, E.J. Prebys, C. Bamber, S. Boege, T. Kotseroglou, A. C. Melissinos, D.D. Meyerhofer, W. Ragg, D.L. Burke, R.C. Field, G. Horton-Smith, A.C. Odian, J.E. Spencer, D. Walz, S.C. Berridge, W.M. Bugg, K. Shmakov and A. W. Weidemann, Phys. Rev. Lett. 76, 3116 (1996).

[8] C. Bamber, S.J. Boege, T. Koffas, T. Kotseroglou, A.C. Melissinos, D.D. Meyerhofer, D.A. Reis, W. Ragg and C. Bula, Phys. Rev. D 60, 092004 (1999).

[9] H. Hu, C. Mueller and C.H. Keitel, Phys. Rev. Lett. 105, 080401 (2010).

[11] E. N. Nerush, I. Yu. Kostyukov, A.M. Fedotov, N.B. Narozhny, N.V. Elkina, and H. Ruhl, Phys. Rev. Lett. 106, 035001 (2011).

[12] A.I. Titov, B. Kampfer, H. Takabe and A. Hosaka, Phys. Rev. A 87, 042106 (2013).

[13] O.J. Pike, F. Mackenroth, E.G. Hill and S.J. Rose, Nature Photonics. 8, 434 (2014).

[14] B. King and H. Ruhl, Phys. Rev. D 88, 013005 (2013).

[15] A. Di Piazza, Phys. Rev. Lett. 113, 040402 (2014); Phys. Rev. A 91, 042118 (2015)

[16] M.J.A. Jansen and C. Mueller, Phys. Rev. A 88, 052125 (2013).

[17] M.J.A. Jansen and C. Mueller, Phys.Rev. D 93, 053011 (2016).

[18] M.J.A. Jansen and C. Mueller, Phys. Lett. B 766, 71 (2017).

[19] O.W. Greenberg and S.S. Schweber, Nouvo Cimento 8, 378 (1958).

[20] S.S. Schweber, "An introduction to relativistic quantum field theory" (Harper & Row, New York, 1962).

[21] R. Walter, Nouvo Cimento 68 A, 426 (1970).

[22] Q.Z. Lv, S. Norris, R. Brennan, E. Stefanovich, Q. Su and R. Grobe, Phys. Rev. A 94, 032110 (2016).

[23] R.E. Wagner, M.R. Ware, B.T. Shields, Q. Su and R. Grobe, Phys. Rev. Lett. 106, 023601 (2011).

[24] R.E. Wagner, M.R. Ware, Q. Su and R. Grobe, Phys. Rev. A 82, 032108 (2010).

[25] T. Cheng, C.C. Gerry, Q. Su and R. Grobe, Europhys. Lett. 88, 54001 (2009).

[26] R.E. Wagner, Q. Su and R. Grobe, Phys. Rev. A 82, 022719 (2010).

[27] C. Lisowski, S. Norris, R. Pelphrey, E. Stefanovich, Q. Su and R. Grobe, Ann. Phys. 373, 456 (2016).

[28] Q.Z. Lv, S. Norris, R. Pelphrey, Q. Su and R. Grobe, Comp. Phys. Comm. 219, 1 (2017).

[29] L. Allen and J.H. Eberly, "Optical resonance and two-level atoms" (Dover, New York, 1975).

[30] C.C. Gerry and P.L. Knight, "Introductory quantum optics" (Cambridge University Press, Oxford, 2004).

[31] J.D. Bjorken and S.D. Drell, "Relativistic quantum fields", (McGraw-Hill, New York, 1965).

[32] M.E. Peskin and D.V. Schroeder, "An introduction to quantum field theory" (Westview Press, 1995).

[33] E.V. Stefanovich, Ann. Phys. 292, 139 (2001).

[34] R.E. Wagner, Q. Su and R. Grobe, Phys. Rev. A 88, 012113 (2013); E.V. Stefanovich, R.E. Wagner, Q. Su and R. Grobe, Laser Phys. 23, 035302 (2013); Q.Z. Lv, E. Stefanovich, Q. Su and R. Grobe, Laser Phys. 27, 105301 (2017).

[35] Dirac, P.A.M. Proc. Royal Soc. A 114, 243 (1927); E. Fermi, "Nuclear physics" (University of Chicago Press, Chicago, 1950).

[36] E.V. Stefanovich, Int. J. Theor. Phys. 35, 2539 (1996).

[37] M.I. Shirokov, Int. J. Theor. Phys. 43, 1541 (2004).

[38] E.V. Stefanovich, "Relativistic quantum theory of particles" Vols. I and II (Lambert Academic Publishing, Saarbrücken, 2015).

[39] B.T. Shields, M.C. Morris, M.R. Ware, Q. Su, E.V. Stefanovich and R. Grobe, Phys. Rev. A 82, 052116 (2010).

[40] M.D. Schwartz, " Quantum field theory and the Standard Model" (Cambridge University Press, 2008).

[41] B. Thaller, "The Dirac equation", (Springer-Verlag, Berlin, 1992).

[42] W. Greiner, B. Muller and J. Rafelski, "Quantum electrodunamics of strong fields" (Springer-Verlag, Berlin, 1985).

[43] T. Cheng, E.R. Gospodarczyk, Q, Su and R. Grobe, Ann. Phys. 325, 265 (2010).

[44] G.B. Arfken and H.J. Weber, "Mathematical methods for physicists" (Academic Press, San Diego, 1995).

[45] H.M. Faisal, " Theory of multiphoton processes" (Springer, Berlin, 1987).